minerals

MDPI

Article

Mapping New IOCG Mineral Systems in Brazil: The Vale do Curaçá and Riacho do Pontal Copper Districts

Sérgio Roberto Bacelar Hühn [1,*], Adalene Moreira Silva [2], Francisco José Fonseca Ferreira [3] and Carla Braitenberg [4]

1 Department of Geology, Universidade Federal do Ceará-UFC-Campus do PICI, Fortaleza 60440-554, Brazil
2 Instituto de Geociências, Universidade de Brasília, Brasília 70910-900, Brazil; adalene@unb.br
3 Laboratório de Geofísica Aplicada, Universidade Federal do Paraná, Curitiba 81531-980, Brazil; francisco.ferreira@ufpr.br
4 Department of Mathematics and Geosciences, University of Trieste, 34149 Trieste, Italy; berg@units.it
* Correspondence: sergio.bacelar@ufc.br

Received: 5 September 2020; Accepted: 24 November 2020; Published: 30 November 2020

Abstract: The Vale do Curaçá and Riacho do Pontal copper districts are located within the northern part of the Archaean São Francisco Craton and represent two pulses of mineralization. The copper districts have been identified as Iron-Oxide-Copper-Gold (IOCG) classes of deposits. An older metallogenic event associated with the Caraíba copper deposit, which is located in the Vale do Curaçá district, is related to Palaeoproterozoic (ca. 2 to 2.2 Ga) hydrothermal processes. A younger Neoproterozoic (ca. 750 to 570 Ma) episode of volcanism and associated plutonism is represented by the Riacho do Pontal mineral district. Seismic tomography data from across east-central Brazil show that the multiage Carajás province and Vale do Curaçá and Riacho do Pontal copper districts sit along either side of a prominent NW-trending upper lithospheric high-velocity zone. The edges of the high-velocity zone point to long-lived subparallel transcrustal structures that have been the focus of multiple reactivations and copper mineralization events. Regional gravity and magnetic maps show that the Vale do Curaçá copper district extends over an area greater than 110 km by 22 km. The magnetic and gravity values show significant variations correlated with this area. The district includes high gravity values associated with the Caraíba copper mine (>−35 mGal), which has a greater density (3.13 g/cm^3) than the nonmineralized host rock density (2.98 g/cm^3). The gravity anomaly signature over the Riacho do Pontal copper district is characterized by a 40-km long NW–SE trending Bouguer gravity low. The Ria4 occurrences of the Riacho do Pontal copper district are situated in these regional low-gravity domains. Data from regional airborne magnetic and ground gravity surveys were inverted to obtain a 3D magnetic susceptibility and density model, respectively, for the known districts. The results show that the Caraíba deposit is characterized by a both dense and magnetic source showing structural control by thrust shear zones. The 2D and 3D geological models show two main NNW prospective trends. Trends I and II have a sigmoidal shear shape and are positioned in the contact zone between domains with high magnetic susceptibility (SI > 0.005) and density > 0 g/cm^3). Trend I is 40 km × 10 km in size and hosts the Caraíba, Surubim, and Vermelho copper mines and other minor deposits. The results obtained from the 3D magnetic inversion model for the region of the Riacho do Pontal district show weak magnetic anomaly highs extending along a NW–SE magnetic gradient trend. The gradient is related to mapped shear zones that overprint older and deeper NE–SW features of the São Francisco cratonic root. The area includes high gravity values associated with the Caraíba copper deposit, which has a greater density (3.13 g/cm^3) than the nonmineralized host rock density (2.4 g/cm^3).

Keywords: 3D data integration; IOCG; Palaeoproterozoic; gravimetric and magnetic inversion; Riacho do Pontal; Brazil

1. Introduction

World-class IOCG (Iron Oxide Copper-Gold) deposits express their metallogenic footprint in different tectonic settings through variable volumes of associated alteration and metal endowments, which can be geophysically sensed [1–4]. IOCG mineralization is often controlled by shear system zones and involves high concentrations of magnetite and/or hematite. Magnetic and gravity signatures related to magnetite- and hematite-rich copper ore zones have led the mining community and other researchers to use these data as an effective exploration tool to find new IOCG deposits [5–8]. Frequently, the geometry and structural control of mineralized trends are related to secondary structures and transtensional sites [9–11]. The orebodies are structurally controlled by stretching lineations associated with the shear zone. These important geologic features of IOCG mineralization are often expressed in physical property changes related to density, magnetization, and seismic velocities at a wide range of scales [1,5,10].

Geologic characteristics of the world-class Carajás IOCG deposits are distinct and show a complex interplay between geologic structures, fluid flows, and forms of hydrothermal alteration [12–24]. For example, the flow of mineralized fluids along regional shear zones is responsible for the "sigmoidal-shape" structural pattern and magnetic signature of the Carajás province and Vale do Curaçá district [6,14,20,25].

The Vale do Curaçá and Riacho do Pontal copper districts host copper as the primary commodity along with Au, Fe, and Cr and other metals [26,27]. Early studies characterized the copper deposits as magmatic. According to Lindenmayer et al. [13,14], mineralization is exclusively hosted in orthopyroxenite. High concentrations of sulfides, however, can also occur in norite- and biotite-rich shear rocks and in calcsilicate rocks. Recently, new geologic [24,26–29], tectonic [26,30], isotopic, and geochemical [27] studies have shown evidence that copper mineralization is related to the diverse family of IOCG deposits. In the last 10 years, high-resolution airborne geophysical surveys have been completed. This geophysical effort has motivated new exploratory campaigns in both districts. However, despite an increase in modern airborne geophysical coverage and geologic mapping, the rate of the discovery and identification of new IOCG deposits remains low. This low discovery rate is partly due to the absence of a modern mineral systems approach followed by a systematic exploration program that involves higher density exploration drilling. Additional challenges exist because shallower deposits have been discovered, and presently, major efforts are focused on deeper exploration below different types of cover. Outcrop deposits have already been discovered. The new targets are located deeper within and/or below the cover.

Both the Vale do Curaçá and the Riacho do Pontal copper districts can be considered among the most important areas for IOCG prospectivity in Brazil [24,26,27]. Globally, IOCG deposits are a significant source of base and precious metals, which is key to supporting and expanding economic growth. In particular, the Vale do Curaçá copper district, which occupies an area of approximately 2000 km^2, is one of the most significant mining districts in Brazil, having produced 30 kt of copper in 2018. Approximately 300 copper occurrences and prospects have been mapped. The district includes a total of 42.4 Mt @ 1.71% copper [30–32]. The most productive copper deposits in the Vale do Curaçá are Caraíba-Pilar (24.8 Mt @ 1.9% copper), Vermelhos (4.52 Mt @ 3.4% copper, underground) and Surubim (4.5 Mt @ 1.04% copper) [32].

Despite these important metal endowments, there is a lack of knowledge that would provide broad insight into how the deposits formed and concerning the larger mineral systems that were active during their emplacement. A previous study [24] used multiparameter geologic and geochemical remote sensing and airborne geophysical data to statistically identify new areas of IOCG prospectivity

related to shallow mineralization along the northern border of the São Francisco Craton (Figure 1). Areas of known mineralization and targets of new prospectivity were identified in a previous data integration study [24]. The study presented here expands on this previous work in three different ways. First, magnetic and gravity maps are interpreted in concert with new geologic information to map deep crustal and lithospheric controls on copper mineralization. Second, regional magnetic and gravity data are inverted to obtain 3D models of magnetic susceptibility and density, respectively, to understand the concealed geology related to physical property distributions and geometries underlying the districts. Third, seismic tomography data are analyzed to place the Vale do Curaçá and Riacho do Pontal IOCG districts within a tectonic and cratonic framework and to characterize potential lithospheric controls of the mineral provinces. Our objective is to use these approaches to obtain an advanced understanding of the mineral system(s) that controlled the emplacement of the NE Brazil IOCG mineral districts.

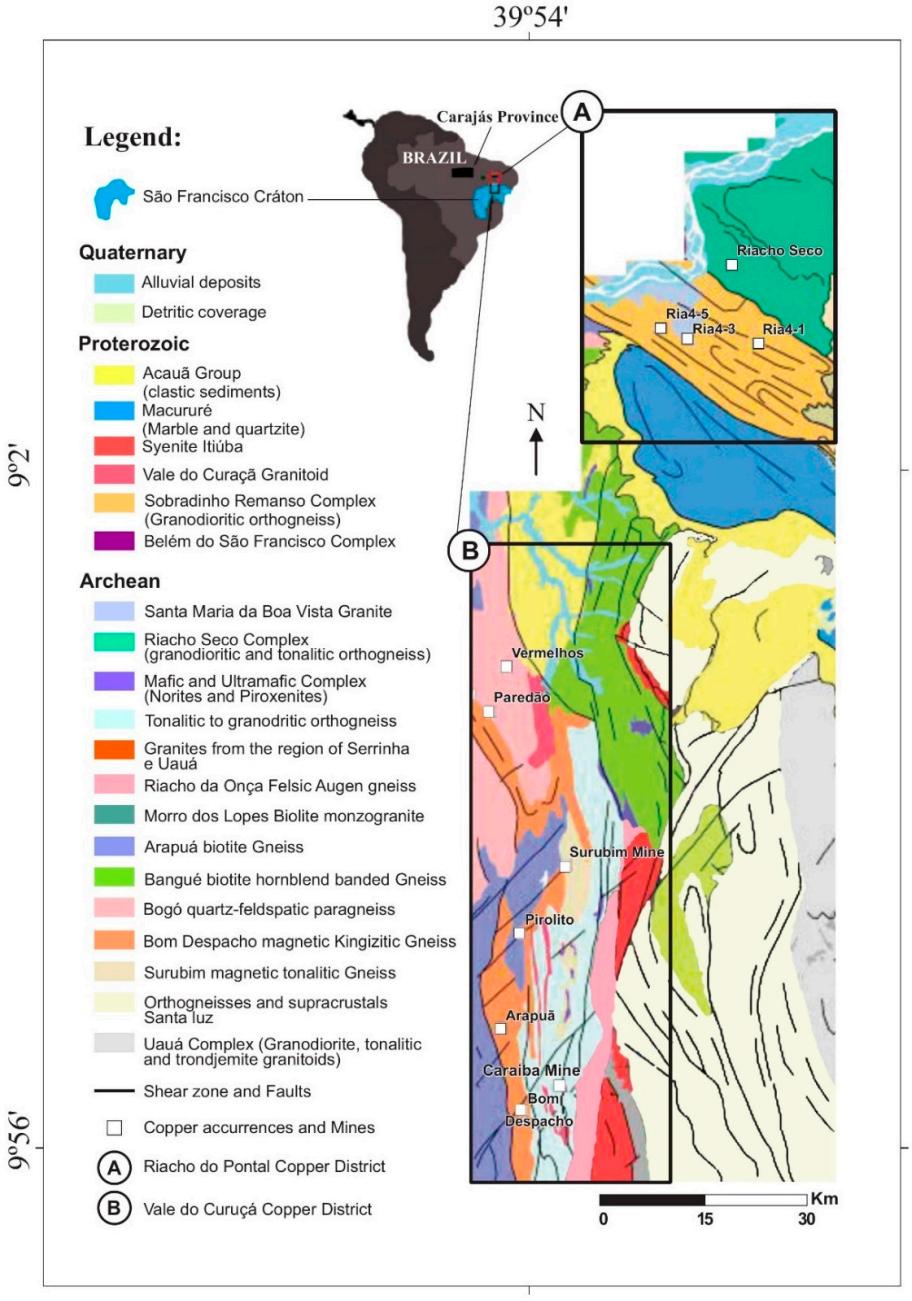

Figure 1. Geologic map showing the study location with (**A**) the Riacho do Pontal and (**B**) the Vale do Curaçá copper districts. Major copper mines and occurrences are shown [20,27,31].

Purpose and Scope

The purpose of our study is to synthesize available regional magnetic, gravity, and seismic tomography data with geologic information to evaluate the 2D and 3D geologic and tectonic setting of the Vale do Curaçá and Riacho do Pontal IOCG districts. An overarching goal of our study is to develop a better understanding of the deep crustal and lithospheric structural controls for Palaeoproterozoic and Neoproterozoic mineralization events.

2. Geologic Setting and Mineralization

2.1. Classification as IOCG Deposits

Early studies of the Caraíba copper mine within the Vale do Curaçá district emphasized orthomagmatic processes as responsible for the genesis of copper mineralization [13,14,30]. noted that the unusual aspects of the Caraíba deposit shared similarities with other copper deposits of magmatic origin [33], including (a) the presence of primary sulfides such as bornite and chalcopyrite; (b) the presence of large amounts (>50 wt %) of magnetite; (c) a high Cu/Ni ratio (~40); and (d) orthopyroxenites with abundant biotite related to shear zones. The importance of metasomatic processes in the genesis of the Caraíba deposit was initially suggested by Rocha et al. [34] and more recently confirmed by Teixeira et al. [20], who proposed that copper deposits in the Vale do Curaçá copper district are analogous to other IOCG deposits worldwide.

Early studies fulfilled by several authors [35,36] on the copper deposits in the Riacho do Pontal district show that they were characterized as the volcanogenic massive sulphide (VMS) type. In the region of Riacho Seco. The following criteria have been used to classify copper mineralization in the Riacho do Pontal district as IOCG deposits [24,28]: (a) strong association with potassic and albite alteration; (b) copper ore that is hydrothermal and epigenetic, which is closely associated with shear zones; (c) the presence of hydrothermal iron oxides spatially and temporally related to copper orebodies; (d) mineralization that is not spatially related to proximal granites; and (e) magnetite or hematite (hydrothermal iron > 10%; [7,8]).

2.2. Palaeoproterozoic Vale do Curaçá Copper District

Since the beginning of the last century, the Vale do Curaçá copper district (B in Figure 1) has been the focus of intense geologic mapping and exploration activity. During the 1970s, a mineral exploration boom occurred in this region. The focus of the exploration program was on copper in volcanic-hosted massive sulfide (VMS) mineralization [37,38] in greenstone belts and copper mineralization hosted in mafic-ultramafic layered complexes [14,31,39]. The exploration activities led to the discovery of the Caraíba mine, which is the largest mine in the district. In addition, a series of copper deposits and occurrences in the Vale do Curaçá district were discovered. Approximately 300,000 m of drilling has taken place in the mining district [40].

The geology of the Vale do Curaçá copper district (B in Figure 1) consists mainly of rocks belonging to the Itabuna-Salvador-Curaçá Orogen (ISCO). The ISCO is located east of the Gavião and Jequié blocks and west of the Serrinha block (Figure 2) and represents an 800 km long belt of Archaean to Palaeoproterozoic high metamorphic grade granulitic rocks [20,41]. These rocks were deformed and metamorphosed due to the collision of the Gavião, Jequié, and Serrinha blocks [20,41–43]. The ISCO is a Rhyacian to Orosirian orogenic belt resulting from the collision of Archaean blocks in the range of ca. 2 to 2.2 Ga [26,44]. This was followed by deformation with high metamorphic grade and syntectonic granites [45]. A SHRIMP U/Pb age of 2695 ± 12 Ma was obtained for granulitic rocks of the Caraíba complex [20] and a U/Pb age of 2072 Ma was found for the metamorphic event [45]. The mafic-ultramafic complex should have mafic-ultramafic intrusions of two different ages (2695 Ma and 2580 Ma).

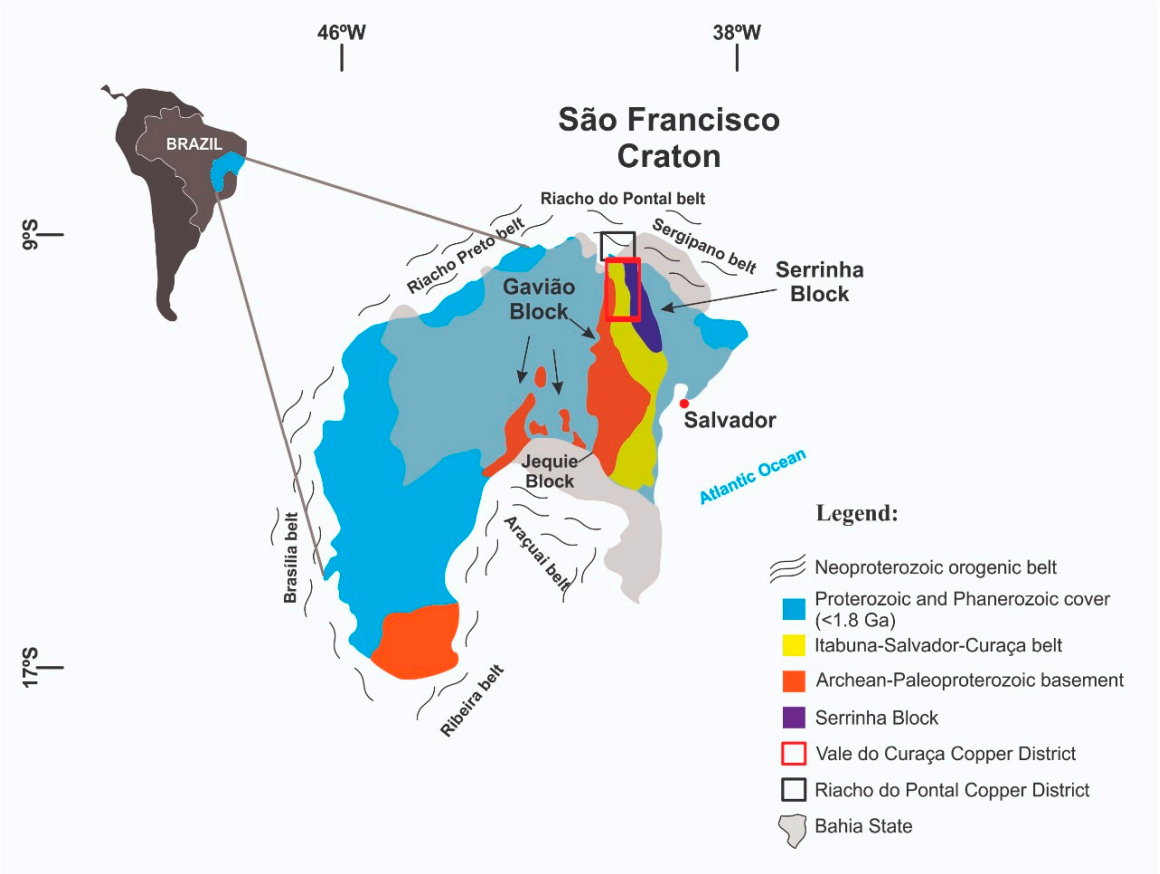

Figure 2. Simplified geologic map of the São Francisco Craton showing the locations of the Riacho do Pontal and Vale do Curaçá copper districts. Both districts are situated on the northern edge of the SFC in contact with Borborema province. (Modified from [26]).

The specific geology of the Curaçá copper district comprises the Tanque Novo and Caraíba complexes. The Tanque Novo complex consists of Bom Despacho, Arapuá, Surubim, and Bogó gneissic rocks [13] composed mainly of feldspathic quartz gneiss, cordierite-garnet-biotite gneiss, amphibolite, and magnetite (quartzite)-rich rocks. The Caraíba complex contains tonalite to granodiorite bodies. A series of mafic-ultramafic bodies individually intruded into the supracrustal rocks. These rocks have undergone episodes of deformation, metamorphism, and related granitic intrusion. The U/Pb SHRIMP ages of ultramafic rocks within the Caraíba mine show that the rocks formed at ca 2580 ± 10 Ma [45]. Field relationships show that the Itiúba syenite is younger than the Medrado gabbro. Importantly, Itiúba syenite is a syn tectonic to shear zone of 2084 ± 9 Ma. This age is also related to copper mineralization situated along shear zones [26,46].

Shear zones have been mapped along the Vale do Curaçá district and are often marked by intense biotite-rich rocks related to mylonitic rocks. These zones are characterized by two phases of progressive deformation [34,46]. (a) The first phase (D1) involved transpressive thrust structures showing convergence to the west. The associated metamorphism occurred in the amphibolite to granulite facies. (b) The D2 phase was related to strike-slip shear zones with N–S isoclinal folds and penetrative vertical shearing structures. Kinematic studies indicate that D1 was overprinted by sinistral strike-slip shear zones [26,47]. These shear zones were responsible for the positioning of mylonitized granites and the intense fluid flux. The shearing process destroyed the preexisting fabric. The foliation of shear zones has a strike of 350° and dips towards SE at 45° to 75°. The main mineralization event in the Vale do Curaçá district occurred between ca 2050 and 2010 Ma [26,29].

Geology of the Caraíba Mine

The geology of the Caraíba mine is well marked by the contact between orthogneiss (G2) and mafic-ultramafic rocks. Frequently, biotite has been mapped along N–S trending geologic contacts. The supracrustal rocks include banded gneiss, diopsidite, forsterite marbles, garnetiferous mafic granulite, biotite-schist, and iron formations [14].

The Caraíba orebody is hosted mainly in mafic-ultramafic complexes [20,34] with recognized hydrothermal calcic-ferric alteration related to copper-ore zones. More recent work shows early (2580 ± 10 Ma; [45]) orthomagmatic mineralization overprinted by a later hydrothermal event that produced IOCG mineralization at ca 2 Ga [20,29,36]. Studies conducted by [46–48] show evidence of structural control at the Caraíba mine.

Ore minerals at Caraíba include chalcopyrite, bornite, and chalcocite, which are usually associated with magnetite. Intercumulus crystals of disseminated chalcopyrite, bornite, and magnetite grown in the interstices of pyroxenes and amphiboles constitute the primary (magmatic) mineralization. Minerals associated with hydrothermal alteration include biotite, microcline, epidote, chlorite, magnetite, and quartz [36]. Ore often occurs as veining or magnetite hydrothermal breccia. Magnetite sometimes occurs in equilibrium with spinel. Frequently, ilmenite exhibits replacement by chalcopyrite, bornite, and magnetite, especially when the host rock is biotite mylonite. Magmatic ilmenite is replaced by ilmenite hydrothermal. The latter IOCG system is richer in copper, highly magnetic, and dense.

2.3. Geology of the Neoproterozoic Riacho do Pontal Copper District

More than twenty copper occurrences have been found in the Riacho do Pontal region (A in Figure 1; [26]). Geologically, these occurrences are mostly located in the contact zone between the Borborema province and the San Francisco craton (Figures 2 and 3). The area includes a small slab of the ca. 750 Ma to 570 Ma Brasiliano collisional zone, which developed during the convergence of Neo- to Mesoproterozoic terrains with the São Francisco craton. Copper occurrences are structurally controlled by shear zones (Figure 1). The Ria4 occurrences and Riacho Seco deposit (Figure 1) are the main copper occurrences in the district. The drill hole intercepted a mineralized zone (0–26 m) related to biotite-malachite (after cpy; 1–3%) parallel to mylonitic foliation.

Several alteration types related to hydrothermal processes have been identified in the Riacho do Pontal district [28]. Hydrothermal alteration has led to a pervasive calcic-potassic and calcic-ferric overprint of the host gneisses and migmatites. Early-stage sodic hydrothermal alteration is distal in relation to areas with calcic-potassic and potassic-ferric alteration with a higher strain rate. Hydrothermal alteration processes led to the replacement of metamorphic minerals within banded gneiss with a suite of minerals, including albite, biotite, hematite, and amphibole. These replacement minerals are spatially connected to penetrative shear deformation, and ore zones plunge parallel to stretching lineations along shear zones. Pyrite, chalcopyrite, and chalcocite are related to the main sulfide minerals found in ore zones. Magnetite and/or hematite typically occurs in association with copper ore minerals and constitutes less than 1% of the paragenesis [29].

The Riacho do Pontal belt was overprinted by two main shearing events: (a) D1-thrust shear zones with convergence to the north representing a series of northwest-trending parallel structures related to hydrothermal alteration and mineralization and (b) D2-dextral strike slip shear zones related to multiple reactivation responsible for the strong shearing of paragneissic and orthogneissic rocks. The foliation of shear zones is significantly tilted with a strike of 320° and a dip to the NE at 60° to 75°. Both events were related to transpressive structural regimes.

The Riacho do Pontal Copper District is located at the apex of three orogenic belts (the Riacho Preto, Riacho do Pontal, and Sergipana belts), which are located along the northern border of the São Francisco Craton (Figure 2). The area has been located within the Brasiliano collisional zone (from ca. 750 Ma to 570 Ma), which developed during the convergence of the Neo- to Mesoproterozoic terrains of Borborema Province (Figure 3) with the São Francisco Craton [49]. The suture is marked by a gravity anomaly heavily flanked by anomalous lows (Figure 4b). The positive anomaly corresponds to the

lower crustal uplift of the Borborema province, and the flanking negative anomalies correspond to lower density nappes pushed towards the craton [50,51]. According to [50], supracrustal rocks of the Riacho do Pontal and Sergipana belts were placed over the São Francisco Craton with displacements to the south of the order of 30–60 km [52]. This overlapping structure is observed in both magnetic and gravimetric data with the truncation and displacement of old N–S structures occurring along the border between the São Francisco Craton and Borborema terrain. According to [52], the collisional event was overprinted by transcurrent shear zones.

Figure 3. IOCG provinces and districts situated in Brazil and Africa: main crustal blocks and Neoproterozoic orogenic belts in South America and Africa, including locations of the West Gondwana Orogen (modified after [53–57]).

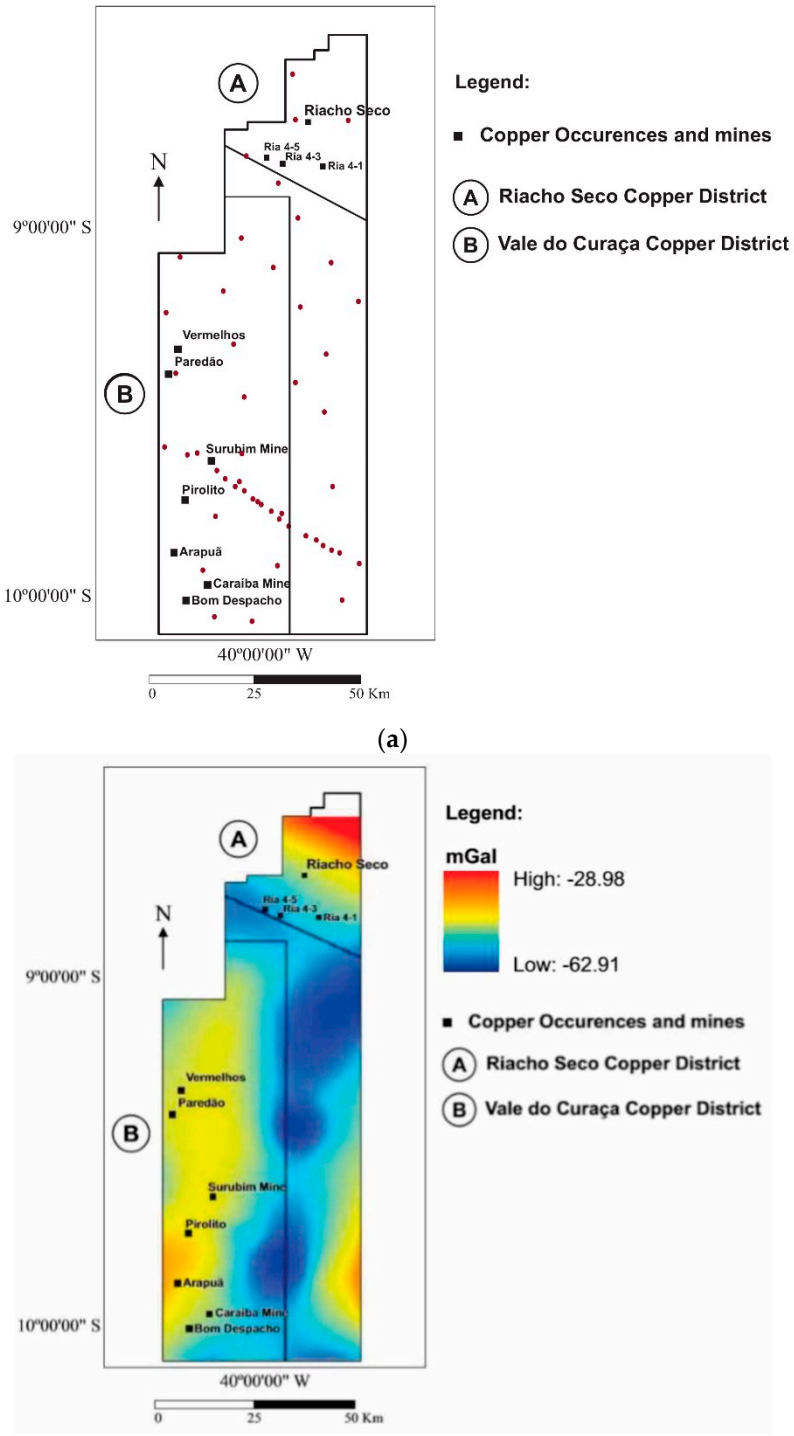

Figure 4. (**a**) Gravity stations and (**b**) Bouguer gravity map for the study area. Major copper occurrences and mines are shown. Block A: Riacho do Pontal district; block B: Vale do Curaça IOCG district.

3. Tectonic Setting

IOCG provinces and districts in Brazil and Africa are mainly situated along the borders of major crustal blocks and in Neoproterozoic orogenic belts (Figure 3). There are at least three IOCG metallogenic provinces with different ages in Brazil, which include the Carajás province (ca 2.72 Ga and ca 2.5 Ga), the Vale do Curaçá district (ca 2 Ga), and the Neoproterozoic (ca 750 Ma–570 Ma) districts of Riacho do Pontal.

4. Data

4.1. Gravity and Magnetic Data

Gravity and magnetic anomaly data over an area of 7500 km^2 were extracted from public databases available from the Brazilian Geological Survey (CPRM) and the gravity data reduced to Bouguer gravity anomalies using procedures described in [50]. A total of 60 gravity points spaced an average of 8 to 15 km distance were extracted from the gravity database and used for this study (Figure 4a). Given the coarse spacing of the gravity data, we expect crustal density sources that occur at depths of 5 km and beyond to be effectively resolved. The gravity data were gridded by applying a minimum curvature algorithm to a 500 m grid (Figure 4b). The gravimetric signature is quite distinct in both districts while the Vale do Curaça Copper District is associated with a higher gravimetric signature, and the Riacho do Pontal Copper District is associated with a lower valued gravimetric domain (Figure 4b).

Airborne magnetic anomaly data were acquired in 2001 as part of the Riacho Seco and Andorinhas Project executed by the Brazilian Geological Survey [58]. Data were collected at a nominal height above ground of 100 m along N–S flight lines spaced 500 m with E–W tie lines every 10,000 m. A total of 48,641 km of magnetic data were collected. The total magnetic field (TMI) flight line data were gridded onto a 250 m grid (Figure 5). Given the flight-line spacing of the magnetic surveys and height at which the magnetic field measurements were observed, we expect to resolve crustal magnetic sources that lie at depths of 400 m and deeper [59]. The horizontal resolution is 200 m.

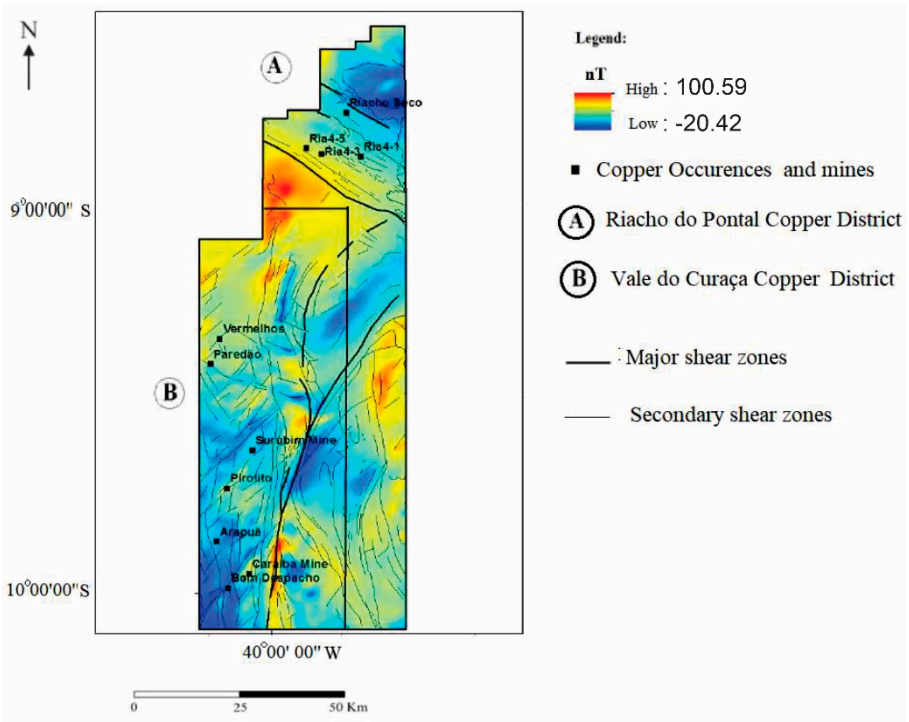

Figure 5. The reduced to pole (RTP) total magnetic intensity (TMI) data upward continued to 1000 m above ground. Major Cu mines and occurrences are shown. Block A: Riacho do Pontal district; block B: Vale do Curaçá IOCG district.

Gradient Functionals Calculated from the Magnetic Data

Several gradient quantities of the magnetic field were calculated from the grid of the TMI to enhance magnetic variations and lineations related to geologic structures, map magnetic signatures of altered and unaltered rocks, and identify magnetic signatures related to deep magnetic sources. The TMI data were reduced to the magnetic north pole (RTP) using an inclination of −20° and declination of −22.31° [60]. The RTP grid was continued upward to 1000 m above the terrain to reduce

noise caused by the low geomagnetic latitude and to enhance the magnetic signatures of deeper sources (Figure 5).

The grid of upward-continued RTP data was used to calculate the tilt angle of the total horizontal gradient (TAHG; [60]). The TAHG transform clearly identifies tracks of high anomaly gradients that map magnetic contrasts related to geologic structures at a range of depths (Figure 6a). Tracks of the TAHG ridgelines, marking major geologic structures, are shown relative to the gravity anomaly map (Figure 6b). The TAHG effectively identifies changes in the prevailing geologic structures as the northern limit of the SFC, where the main strike of the gradient changes from sub-NS orientations to SSW–NNE directions on the SFC and to SE–NW oriented strikes north of the SFC along the Sergipano foldbelt. The SE–NW strike farther north is replaced by more chaotic strike directions when moving northwards out of the foldbelt. Major copper mines Ria 1 to Ria 5 are located in the well-defined SE-NW striking magnetic field anomalies. The copper mineralizations are tied to shear movements and to magnetite and hematite occurrences. It is to be expected that the magnetic anomalies are correlated with the copper mines and have shearing strike directions.

Euler deconvolution solutions [61] were calculated from the grid of the magnetic anomaly data, and depths to magnetic source (structural index = 0) are shown along major shear zones. The structural index = 0 is adequate for detecting the top of a thick slab [62].

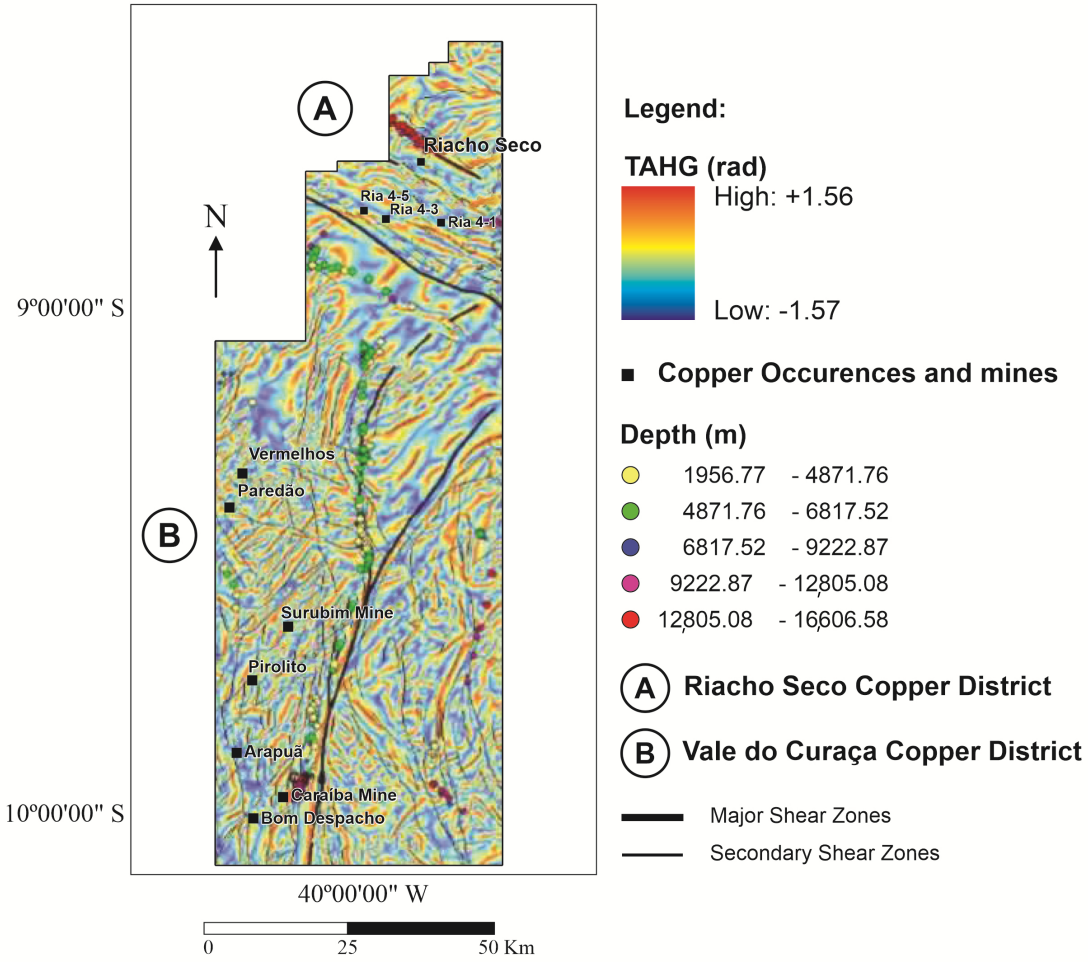

(**a**)

Figure 6. *Cont.*

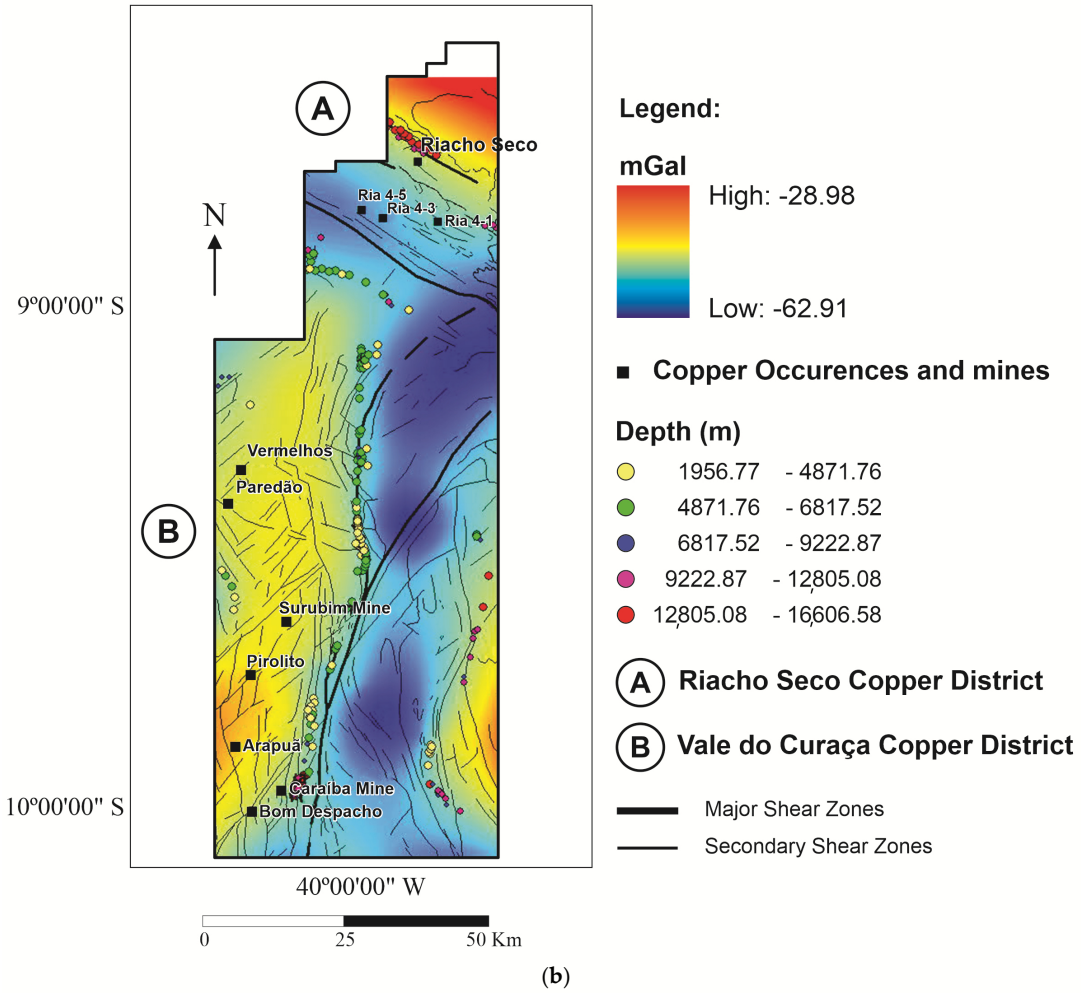

(**b**)

Figure 6. (**a**) Map showing the tilt angle of the horizontal gradient (TAHG) of the RTP magnetic anomaly data [60]. (**b**) Bouguer gravity anomaly map with major and secondary shear structures and TAHG tracks. Both maps include estimates of magnetic structures and their depths to the magnetic source as colored circles. Depths to the magnetic structures were calculated using the Euler deconvolution method [62]. Primary Copper Districts and occurrences are shown. Block A: Riacho do Pontal district; block B: Vale do Curaçá district. The detailed geology of the two studied districts is shown in Figure 1.

4.2. Petrophysical Data

Magnetic susceptibility and density data were acquired from drill cores and surface rock samples. Measurements are provided as susceptibility in SI (susceptibility intensity) $\times 10^{-3}$ and density in g/cm^3. Magnetic susceptibility was measured using a KT10 PLUS S/C susceptibility meter, and rock density was measured by vacuum saturating the samples using a hydrostatic balance. During the field seasons, 33 drill core samples were investigated to determine density and susceptibility from samples collected in the Riacho do Pontal copper district, and 11 rock samples were collected from the outcrops and mines of the Vale do Curaça copper district (Figure 7).

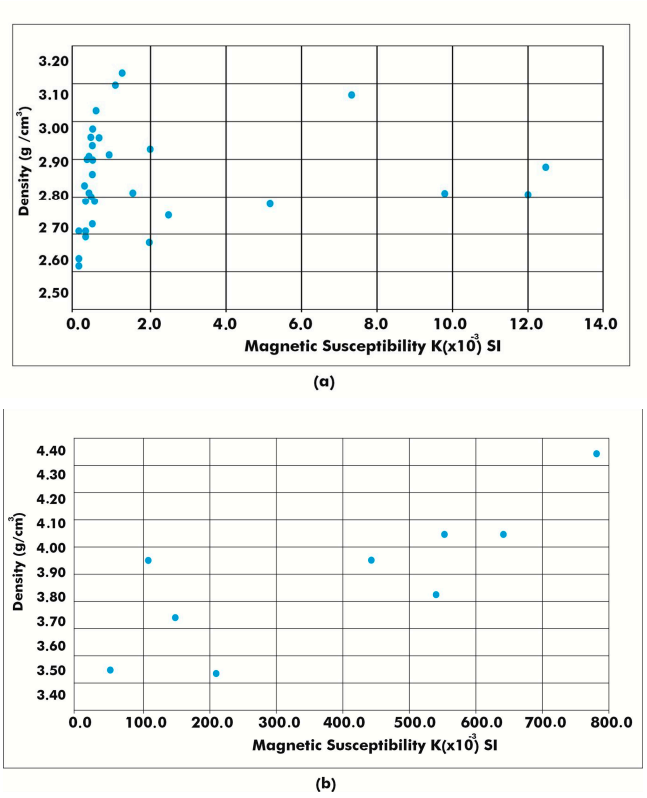

Figure 7. (**a**) Thirty-three samples measured for density and susceptibility taken from exploration drill holes in the Riacho do Pontal copper district, (**b**) 11 samples measured for density and susceptibility from rock samples collected from the outcrops and mines of Vale do Curaça copper district.

The densities found for the Riacho do Pontal copper district are representative of the rock types found in the boreholes, which are gneissic rocks (Table 1).

Table 1. Rock types and depths of samples from the Riacho do Pontal copper district sampled from two drill holes (PCB-RIA4-DH01 and PCB-RIA4-DH02).

PCB-RIA4-DH01	Depth (m)	Rock Type	PCB-RIA4-DH02	Depth (m)	Rock Type
PETRO-01	1.85	Quartz-magnetite-biotite mylonite	PETRO-21	2.75	Amphibole biotite gneiss
PETRO-02	5.50	Quartz vein	PETRO-22	10.60	Quartz vein
PETRO-03	8.70	Biotite mylonite	PETRO-23	14.30	Quartz vein
PETRO-04	10.70	Biotite mylonite	PETRO-24	26.30	Quartz vein
PETRO-05	13.00	Biotite mylonite	PETRO-25	31.80	Quartz vein
PETRO-06	21.00	Biotite mylonite	PETRO-26	45.69	Quartz vein
PETRO-07	25.50	Biotite mylonite	PETRO-27	60.00	Quartz vein.
PETRO-08	32.48	Quartz biotite gneiss	PETRO-28	73.10	Biotite quartz vein.
PETRO-09	67.70	Quartz biotite gneiss	PETRO-29	83.60	Quartz vein
PETRO-10	105.30	Quartz biotite gneiss	PETRO-30	103.50	Quartz vein.
PETRO-11	158.00	Quartz biotite gneiss	PETRO-31	137.00	Biotite quartz gneiss.
PETRO-12	167.80	Quartz biotite gneiss	PETRO-32	148.80	Biotite quartz gneiss
PETRO-13	173.60	Quartz biotite gneiss	PETRO-33	168.10	Biotite mylonite
PETRO-14	189.00	Quartz biotite gneiss	PETRO-34	265.10	Biotite quartz gneiss

The characteristic density and susceptibility values in the two districts are very different, as is the relation between the two quantities. The Riacho do Pontal copper district has quite standard crustal-rock-type densities, with values between 2.6 and 3.1 g/cm^3. For all of the rock samples the magnetic susceptibility is proportional to density, but with two groups of proportionality. A first group is only mildly proportional, with susceptibility varying between 0 and $1.8{\cdot}10^{-3}$ SI, and the other group is highly proportional, with susceptibility varying between 0 and $13{\cdot}10^{-3}$ SI. For the second group the hydrothermal process was responsible for increase of magnetite. The Vale do Curaça

copper district has much higher densities between 3.5 and 4.4 g/cm^3, with much higher proportionally varying susceptibilities values, ranging between 0 and 800·10^{-3} SI. The densities of the Vale do Curaça copper district are typical of mafic and ultramafic rocks, rather than crustal type rocks. In the area the metamorphism has overprinted the ultramafic rocks, transforming them into granulites. The IOCG hydrothermal process in the shear zones increases the magnetization through deposition of magnetite in veins associated with copper mineralization.

4.3. Geologic Data

A compilation of data from the Brazil Geological Survey (CPRM) was used as a geological base map [20]. Supplemental geologic information, including structural and image interpretation data (Landsat 8), was collected for this study along secondary roads, resulting in an additional 300 geological observations [28]. Geologic sections along selected profiles were developed to better understand the structural setting of the area.

4.4. Seismic Tomography

Seismic tomography data have been collected for an area covering east-central Brazil [63,64]. The seismic velocity model which emerged from that study were provided to us by Minerals Targeting International Pty Ltd. and were extracted from a database produced as part of the Global Lithospheric Architecture Mapping (GLAM) Project [65] and refer to the methodology used for the model of [63]. The tomographic image shows the S-wave velocity (Vs) of the Carajás IOCG province, Riacho do Pontal and Vale do Curaçá copper districts in Brazil [63]. The data were used to determine seismic properties related to the lithosphere underlying major IOCG provinces in Brazil (Figure 8). The data represent a model of average seismic velocities at the depth slice of 0–100 km [63]. Our studied area is inboard of a relatively high velocity region, bordered eastwards by a low velocity region. The high-velocity region presumably indicates the cratonic area, with the lower velocity region demarcating the craton limit.

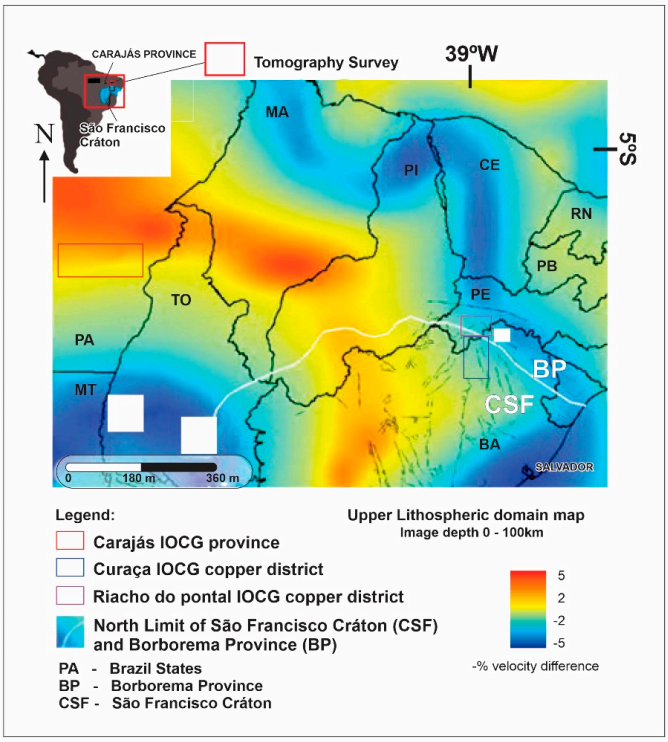

Figure 8. Tomographic image representing seismic S-wave velocity (Vs) of the Carajás IOCG province, Riacho do Pontal and Vale do Curaçá copper districts in Brazil [63–65]. The figure shows a 0–100-km tomographic depth slice. Red to orange colors denote high S-wave velocities (Vs), and blue-green colors denote low Vs values.

5. Methods

5.1. 3D Magnetic and Gravity Inversion Models

The magnetic potential method is sensitive to the magnetic properties of the rocks in terms of residual and induced magnetization. However, applications of this practice have been limited by conventional assumptions that rock magnetization is dominated by induced magnetization and that the magnetization direction is aligned with the geomagnetic field [66]. Modeling the magnetization vector direction and strength using magnetization vector inversion (MVI) has challenged these conventions, and MVI modeling has become an important exploration tool in the mining industry [66]. VOXI Earth Modelling is an Oasis Montaj cloud and clustered computing package that allows the inversion of geophysical data in 3D [66,67]. It uses a Cartesian Cut Cell (CCC) and the algorithm has been simplified by Ellis and MacLeod [67] in order to represent geological surfaces with better accuracy. VOXI Earth Modelling is an Oasis Montaj cloud and clustered computing package that allows the inversion of geophysical data in 3D [66,67]. It uses a Cartesian Cut Cell (CCC) and the algorithm has been simplified by Ellis and MacLeod [67] in order to represent geological surfaces with better accuracy.

Let us begin with the very general assumption that the magnetic properties of the earth can be represented by volume magnetization [68]. We make no assumptions about whether the source of this magnetization is induced or remanent [66,68].

Magnetic and gravity data were inverted to create 3D models of magnetic susceptibility and density, respectively, of selected areas of the two studied copper districts to better understand the anatomy of the crust underlying them. The three-dimensional models were integrated with other project data using a multicore cloud-based computing platform.

5.2. 3D Magnetic Inversion

The grid of total field magnetic anomaly data was inverted to create a 3D magnetic susceptibility model using the MVI method developed by [67] and employing software available from the Geosoft Oasis software package [66,68]. The MVI method is a particularly effective inversion methodology to use in areas of low geomagnetic latitude and in geologic environments where little is known about the remanent magnetization of the rocks under study [66].

No palaeomagnetic studies have been conducted on the rocks within these copper districts. The method assumes that the magnetic signal observed at the surface is associated both with varying susceptibility contrasts and with the varying direction of magnetic field magnetization, which allows one to verify the presence of remanence. In the end, we conclude that remanence is not present.

Voxels for the magnetic inversion were set to 250 m (x) × 200 m (y) × 250 m (z). Model inputs included petrophysical properties, surface geology, and structural information as qualitative constraints.

5.3. 3D Density Inversion

VOXI MVI modeling is a Geosoft Oasis Montaj cloud and clustered computing module used for the inversion of ground gravity data. The Geosoft package uses a cartesian cut cell (CCC) and an iterative reweighting inversion algorithm [67,68]. The algorithm has been simplified by [65,66] and represents geological surfaces with good accuracy. For the gravity models, voxels sized 250 m × 250 m × 250 m were used.

The model used topography to represent the top of the model and a 5000-m depth to constrain the bottom surface of the model. The Z voxel cell size follows a logarithmic progression with depth. The acceptable absolute error level for all models was set to 0.02 mGal. A linear trend background was removed from the input gravity grid to facilitate the modeling process and avoid generating erroneous results and undesirable edge effects. We use the Bouguer gravity field instead of the isostatic anomalies, because in the specific inversion areas, the topography is flat.

6. Results

6.1. Gravity and Magnetic Signatures

6.1.1. Vale do Curaçá District

Gravity anomaly signatures over the Vale do Curaçá copper district (Figure 6b) show that the district is underlain by rocks with high densities in contrast with those surrounding it. The district is located within an elongate 110 km × 22 km long N–S trending gravity high that occurs over rocks related to the Bom Despacho gneiss, Surubim gneiss, Banguê gneiss, mafic and ultramafic complex and tonalitic to granodioritic orthogneiss (Figure 1). In this study, density measurements were made from these units, including gneissic-granite, mylonitic, and pyroxenite rocks, which have average densities of 2.78, 3.1, and 3.3 g/cm^3, respectively (Figure 7b). The lower gravity anomalies surrounding the gravity high are associated with the following units: Riacho da Onça augen gneiss and the Acauã Group. The densities measured from these units are generally lower and range from 2.65 to 3.0 g/cm^3. The gravity low is hardly to be expected to be due to an isostatic compensation of topography, as there are little variations of topography.

The mines of Caraíba, Surubim, and Vermelhos and other copper occurrences are located in a region where rocks are widely affected by granulite-facies metamorphism, and strong hydrothermal processes which show a more positive gravimetric region situated on the eastern portion of the Vale do Curaçá.

The mines of Caraíba, Surubim, and Vermelhos and other copper occurrences are located in the eastern region of the Vale do Curaça district, which includes a relatively higher gravimetric region. Density measurements taken from rocks sampled from ore zones within the Caraíba and Surubin mines show very high average densities of 3.5 to 4.35 g/cm^3. Given the coarse gravity station spacing (Figure 4a), we do not expect anomalies associated with the high-density ore to be resolved in the gravity anomaly map. The ore is comprised of high-density rocks. The ore includes chalcopyrite, magnetite, and bornite associated with hornblende, biotite, apatite, and zircon. Chalcocite and ilmenite are rare [13].

The Vale do Curaçá district sits within a NS magnetic high positioned alongside sets of elongate magnetic lows that record major shear structural episodes and juxtaposed rocks with different magnetic susceptibilities. The magnetic anomaly lows are mapped as gneissic rocks and mafic and felsic dikes. These rocks exhibit weak levels of hydrothermal alteration as shown by outcrop and petrographic studies. Copper mineralization in the Vale do Curaçá district is associated with linear NS-trending magnetic anomalies located along the west side of the Itabuna-Salvador-Curaçá Belt (Figure 1). Late NW magnetic trends are related to hydrothermal alteration (Figures 5 and 6a). Late mafic and felsic dikes show the same trend.

The north- to northeast-trending magnetic anomalies of the Vale do Curaçá copper district correspond to anastomosed structures that have been geologically mapped throughout the district. The NS-trending structures have been overprinted by at least two cycles of shearing [34,46]. These later shear faults are recorded on the TAHG map (Figure 6a).

The copper occurrences and mines in this district, including areas of strong hydrothermal alteration, are associated with magnetic anomalies (TMIs) of ~25.98 to ~100.59 nT (Figure 5). Magnetic susceptibility ranges from 100 to 800 × 10^{-3} (Figure 7b). The magnetic susceptibility of ore zones of the Vale do Curaça copper district is ten times higher than that of the Riacho do Pontal district (Figure 7a,b).

6.1.2. Riacho Do Pontal Copper District

The Riacho do Pontal district sits on a gravity gradient that separates a gravity high to the north from a NW-trending gravity low to the south (Figure 6b). The Bouguer anomaly low is likely related to low-density gneiss that partly outcrops in the Sobradinho Remanso and the southern portion of the Riacho Seco complex (Figure 1). Ria4 copper occurrences within the Riacho do Pontal district are

situated along the edge of the gravity gradient. Densities measured from rocks within the Ria4 mine show that the less altered rocks have densities of 2.7 to 2.78 g/cm^3. Rocks that have been more heavily altered have densities that overlap with those of less altered rocks and range from 2.75 to 3.1 g/cm^3 (Figure 7b).

The northwest trending Bouguer gravity low underlying the Riacho do Pontal district geologically corresponds to the collisional suture zone located between the higher density cratonic block and the lower density crust forming the Riacho do Pontal mobile belt [50,68]. Ophiolite bodies have been mapped in this region [52].

The northeast portion of the Riacho do Pontal copper district is characterized by a more positive gravimetric anomaly with values >−35 mgal. The gravity high corresponds to foliated orthogneissic rocks of the Riacho Seco complex. The Riacho Seco copper occurrences are situated along the gravity gradient, which likely marks a structure that has juxtaposed the denser crust of the craton against the lower density crust underlying the Riacho do Pontal mobile belt. The area of the gravity gradient includes biotite-garnet rich rocks, which occur along shear zones and host a small number of copper occurrences.

In the Riacho do Pontal Copper District, the copper occurrences (Ria4 and Riacho Seco) are not related to high magnetic anomalies. The Ria4 and Riacho Seco occurrences are hosted, respectively, in nonmagnetic gneiss of the Sobradinho Remanso and Riacho Seco complexes. The gneissic rocks are pervasively hydrothermally altered and have a range of magnetic susceptibility of 0.2×10^{-3} SI in less altered rocks to 12.2×10^{-3} SI in more hydrothermally altered rocks. On a regional scale, the NW–SE trending magnetic anomalies overprint longer wavelength NS trending anomalies related to older and deeper parts of the São Francisco Craton [69].

Copper deposits located in the belt of the Riacho do Pontal copper district are mainly situated in zones with or without weak magnetic anomalies (TMI) with intensities below 40 nT (Figure 5).

6.2. 3D Inversion Models

6.2.1. Vale do Curaçá Copper District

The 3D magnetic susceptibility model of the Vale do Curaçá copper district reveals magnetic features corresponding to numerous geologic structures that reflect episodic tectonic activity. The 3D interpretation was built using field geological and structural data. More than 150 geological points were visited, more than 50 thin sections were described, and at least 20 drill holes were observed. Structural data were systematically collected. A series of parallel magnetic trends aligned N–S and dipping 75–85° to the east are overprinted by at least two episodes of NS-trending shear faults (D1 and D2; [20,34,47]). The Caraíba mine is positioned along a NS-trending subvertical shear zone, showing an anastomosing shape in both the horizontal and vertical directions. A series of subparallel N–S shear structures have been active and responsible for multiple reactivation events. N–S shearing magnetic zones are related to thrust shear zones (D1) with convergence to the west and are overprinted by strike slip faults. The D1 and D2 events controlled the distribution of hydrothermal alteration and mineralization. The NE–SW late shear zones are subvertical [20,34,47].

The Caraíba mine bodies are strongly related to magnetic and gravimetric NS trends which are evident when analyzing the inversion results. In Figure 9, the inverted model is represented through the delineation of the body with high magnetic susceptibility, and high-density contrast. We have chosen a discriminant level that allows to represent the increased density and magnetization through positive density contrast values (>0 g/cm^3) and susceptibility values above 0.005 SI. In a 3D rendering the model of these relatively high values is illustrated in Figure 9, where the known shear faults and the position of the Caraiba open pit mine has been included. A characteristic large-scale densification and increased susceptibility is found below the mine, as is expected considering the results concerning the rock properties we have described above, regarding the rocks that encase the IOCG mineralization (Figure 9). We find that the Caraíba mine and Paredão occurrences show a strong relationship to

magnetic anomalies. The other occurrences along the Vale do Curaçá district are not directly related to high gravimetric and magnetic anomalies.

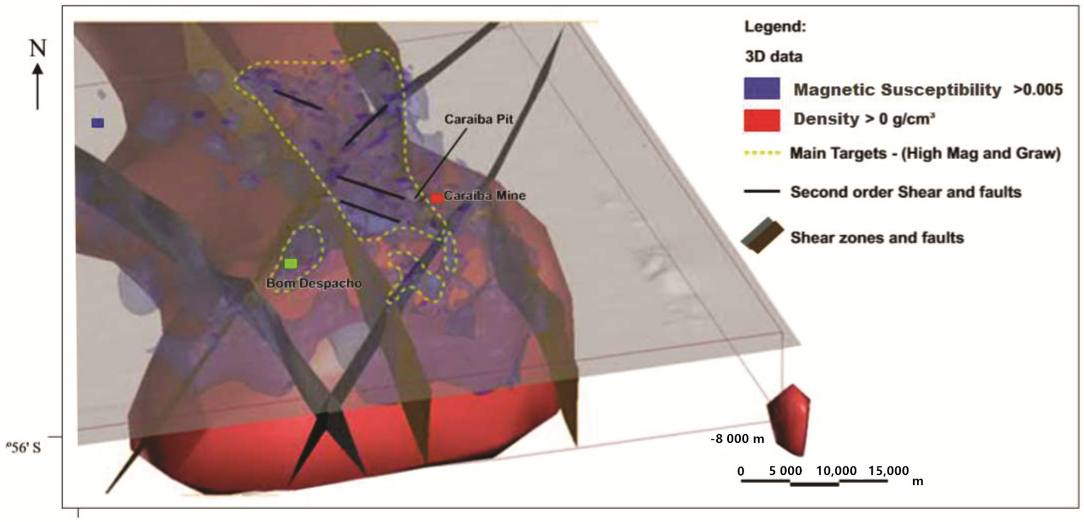

Figure 9. Draping structure and MVI magnetic (SI > 0.005) and density contrast (>0 g/cm^3) inversion onto the terrain surface surrounding the Caraíba mine (Curaçá copper district). In the Vale do Curaçá district, a series of subparallel N–S magnetic trends were found. A great number of magnetic anomalies are related to geological units represented by mafic granulites and granulitic orthogneiss. The dashed yellow area denotes the main target with high potential to host new IOCG orebodies in the Vale do Curaça district.

The host rocks of the Caraíba mine are granulitic orthogneiss and ultramafic bodies. The mine is situated approximately 1 km from the N–S shear zone that was displaced by NW–SE shear zones. Sodic and potassic hydrothermal alterations are mapped along shear zones [20,29]. To demonstrate the inversion results in more detail, we show a section of the model focused on the mine. In a 3D tectonic setting, the mine is intrinsically related to high magnetic susceptibility associated with a positive density anomaly (Figure 10). The orebodies are oriented in a subvertical direction and are controlled by stretching lineation [34]. The model resulting from the inversion of the potential field data is consistent and correlates with the outcropping geology and structural features mapped in the Caraíba mine. In Figure 10, we show a cross section through the model, centered on the mine, and extending 500 m on each side of the mine. The depth extent of the model reaches 8000 m. The blue model shows the relatively high susceptibility, with values being greater than 0.009 SI, whereas the mixed blue and red graph shows the superposition of susceptibility and positive density contrast. The black circle shows the location of the open pit of the Caraíba mine. Shown in grey is the topography, which is completely flat.

The magnetic trends (magnetic susceptibilities > 0.009 SI) are juxtaposed with shear structures and faults with different magnetism intensities (Figure 10). The Caraíba mine correlates with magnetic signatures higher than those of occurrences and deposits situated near the mine.

In Figure 11, the results from the gravimetric and magnetic inversions along an EW profile are shown, with the Caraiba mine in its eastern portion. Highly magnetic (>0.005 SI) and dense (>3.20 g/cm^3) areas are related to rock properties at superficial depths. In the same profiles, at 3000 m depth, magnetization anomalies show continuity up to deeper zones (−8000 m), in the case of density anomalies, in deeper zones (−3000 m), the anomalies do not show continuity: this is interpreted geologically as graffitiated rocks that emerge at shallower depths and probably metasedimentary rocks at greater depths. We find that hydrothermal zones are related to magnetic zones in shear zones, opening the possibility for the continuity of mineralization in deeper zones.

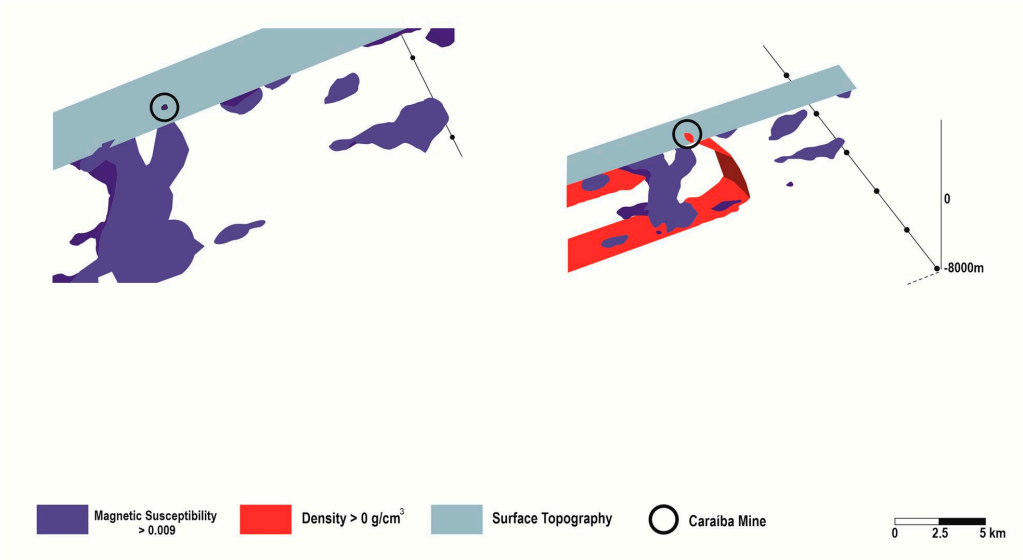

Figure 10. 3D representation of the results from magnetic (susceptibility in terms of >0.009 SI) and gravimetric (density > 0 g/cm^3) inversion integrated for the Caraíba mine. The Caraíba mine is strongly related to susceptibility and density anomalies. It shows potential for continuity in depth in ore zones related to susceptibility and density anomalies along shear traps.

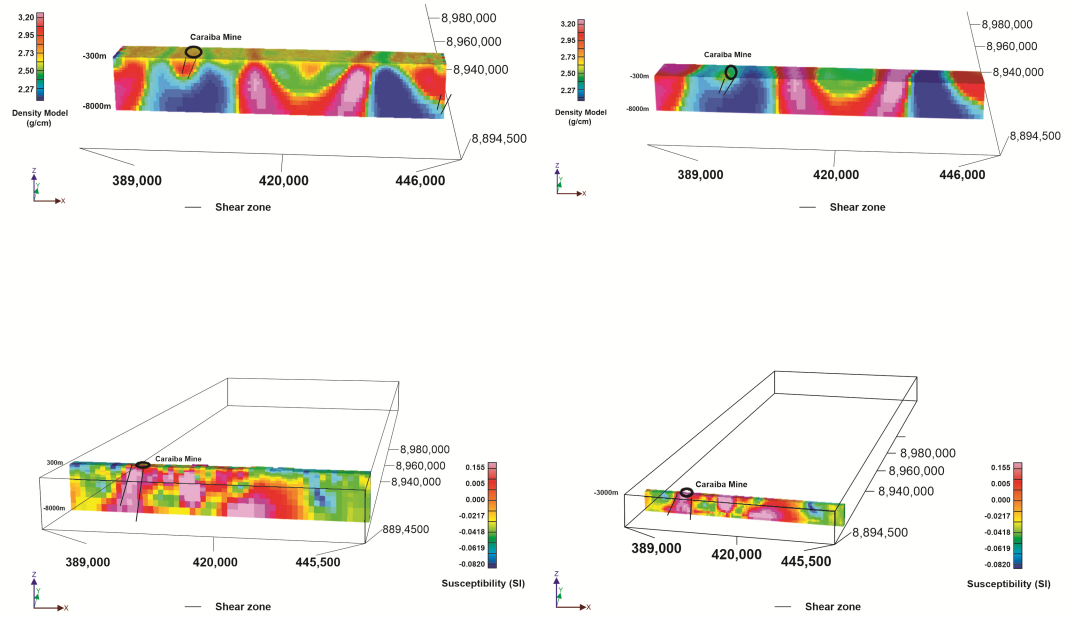

Figure 11. Density and magnetic susceptibility EW profiles in the southern portion of the Valley of the Curaça District, positioned between 300 m and 3000 m depth. Caraíba mine is located in the eastern portion of the area with high density and magnetization values up to 3000 m depth.

Geologically, the regional magnetic trends are related to more intense metamorphic granulitic processes overprinting geological units: the Bom Despacho gneiss and the Surubim, Banguê, and tonalitic to granodioritic orthogneiss. Late NE–SW shear zones are quite common, crosscutting N–S early magnetic trends [20,29,34]. Ore zones from the Caraíba and Surubim mines have a range of magnetic susceptibilities of 400×10^{-3} SI to 750×10^{-3} SI.

In Figure 12 we show the integrated model, with the gravimetric Bouguer values, overlaid on the inverted magnetic and density model. In the 3D view, the red domains are the increased magnetic susceptibility areas, and in grey the positive density contrast areas. Moreover, the faults

are shown. The Caraíba mine is associated with a shear structure, and a high density and magnetic susceptibility zone. It can be seen that the copper occurrences and mines are prevalently associated to increased susceptibility and increased density values. In fact, the occurrences align along the trend I in which we find structures and high density and susceptibility. Moreover, it is found that in the area Central North-East, these conditions are similar, but up to now no occurrences have been explored. In the future, this area should be studied in more detail.

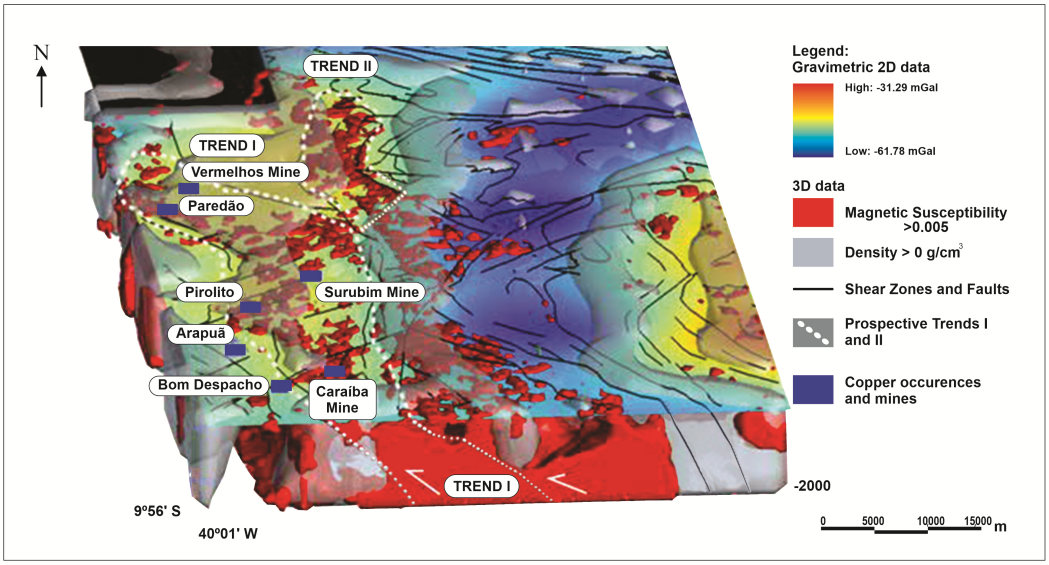

Figure 12. The IOCG mineral system in the region of the Vale do Curaçá Copper District, in regional terms, shows two main prospective trends. The trends are positioned in the contact zone between domains with high magnetic susceptibility (>0.005 SI) and density (>0 g/cm^3) and show contrasts in density and magnetite content.

Three-dimensional magnetic and gravity inversions show two main NNW prospective trends, both with a sigmoidal shear shape. These trends are positioned in the zone of contact between domains with high magnetic (susceptibility > 0.005 SI) and density anomalies (density > 0 g/cm^3) and show contrasts in dense rocks and magnetite content. The trends envelope granulitic rocks but are also the most hydrothermal rocks in the Vale do Curaça district. Trend I is 40 km in length and 10 km in width, hosts the Caraíba, Surubim, and Vermelho mines and other deposits and is the most important trend for host IOCG deposits in the Vale do Curaçá Copper District. Trend II is 15 km in length and 5 km in width. Geologically, these trends are hosted mainly along points of contact between Surubim gneiss, tonalitic to granodioritic orthogneiss, and gabbronorite and/or norite bodies (Figure 12).

The alteration at the Vale do Curaça copper district has a hydrothermal signature characterized by intense potassic-iron alteration indicative of a high temperature system [1,8,10].

Alteration and associated mineralization at the Vale do Curaça Copper District are associated with magnetic and gravity anomalies as observed in other IOCG deposits from Carajás Mineral Province, Brazil; the Gawler Craton, Australia; Kiruna, Sweden; and the Great Bear Magmatic Zone, Canada [1,5,8,10].

6.2.2. Riacho do Pontal District

The 3D magnetic inversion over the Vale do Curaçá copper district shows that the Ria4 prospect and Riacho Seco deposit do not show a correlation with magnetic susceptibilies. Occurrences of copper in the region are positioned at magnetic lows. This observation is explained by the fact that the mineralized zone is related to hematite zones and iron oxide content is low (<2%). The exploratory drilling program (Ria4-DH01) crosscut 32 m @ 1% copper [24,28].

In the Riacho do Pontal district, the copper occurrences are not associated to evident positive density and magnetic susceptibility values. This is coherent with the fact that the rock samples showed gneiss characteristics, with no evident density and susceptibility anomalies. The copper occurrences are associated to the shear faults, but not to increased density and magnetite content. Probably the mineralization and magnetization in the shear zone is much weaker compared to the Val do Curacao district.

The results obtained from magnetic inversions conducted in the region of the Riacho do Pontal copper district show weak magnetic anomalies along a NW–SE trend. The discrete linear magnetic features are related to shear zones. These NW–SE features overlap older and deeper NE–SW features. However, an analysis of Riacho do Pontal district magnetic anomalies in 3D in the Riacho Seco deposit shows a low magnetic anomaly close to the surface and a change in depth (>400 m) to an area with a high magnetic signature (>0.005 SI) (Figure 13). These results allow for the possible development of a continuous model for follow-up research on these deposits as related to deeper magnetic susceptibility anomalies.

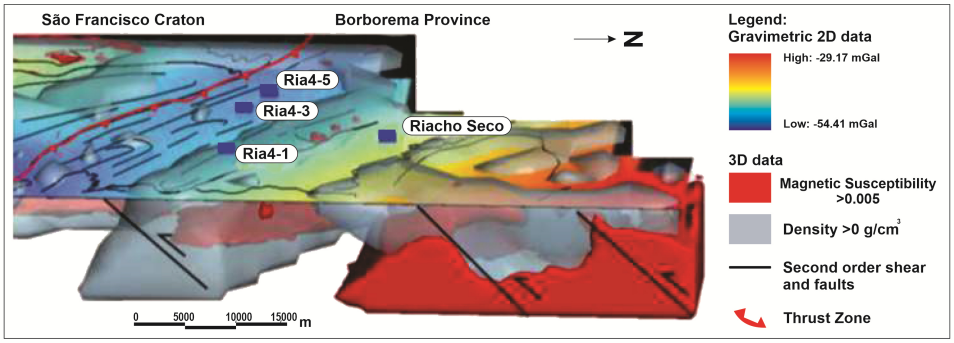

Figure 13. The MVI magnetic gravimetric inversions in the region of the Riacho do Pontal Copper District. Ria4-1, Ria4-3, Ria4-5 and Riacho Seco are the major occurrences at Riacho do Pontal Copper District. In the region of the Riacho Seco Deposit and Riacho do Pontal prospects, the magnetization and density anomalies are weaker (SI > 0.005 and density > 0 g/cm^3) and deeper (>1.5 km).

7. Discussion

7.1. Vale do Curaçá and Riacho do Pontal District IOCG Mineral Systems

Understanding IOCG systems at different scales allows for tracing of some parameters leading to the formation of districts or fertile provinces [6,68,70–76].

More recently, a new generation of ore system exploration models has been developed to take advantage of the massive volume of data available to the exploration industry [76]. Improving exploration competitiveness will be necessary with the more sophisticated integration of different datasets. The challenge remains to decrease the size of exploration areas and increase the success rate of drilling programs [76,77]. Thus, for the Vale do Curaçá and Riacho do Pontal copper districts, the main footprint that shows the ore system signature was identified (Figure 13). The more important geological, structural, geochemical, mineralogical, and petrophysical parameters of these copper districts are summarized below and illustrated in Figure 13.

At a regional scale, large major lithospheric structures control the traps of IOCG mineralizing systems or heat magmas, or fluid flow is frequently evident in gravity and magnetic databases [4]. The outline of the inversion model for Riacho do Pontal obtained using these methods fits well with geological and structural features mapped in the field.

7.1.1. Lithospheric Setting Expressed by the Seismic Tomography Potential

The high zones (in red) on the tomographic map represent high-velocity domains that denote microcontinental blocks (mantle lithosphere domain). They are flanked by low velocity

domains interpreted as the refertilization of the subcontinental lithospheric mantle (SCLM) and/or higher temperatures along fault zones. Frequently, deposits are concentrated along prominent translithospheric structures, particularly in lower-velocity regions (blue) or on the flanks of velocity highs (courtesy of [63,64]).

A world map of the lithosphere produced through the integration of geophysical, geological, and geochemical data shows that approximately 70% of the existing SCLM may be of Archaean origin [63,64]. The implication for an Archaean SCLM is that most preserved Proterozoic crust overlies the older Archaean SCLM variably refertilized and metasomatized by mantle melts associated with convergent margin and mantle plume processes [63,78].

In general, seismic tomography images can show boundaries of cratons and discontinuities related to the SCLM. These discontinuities are favorable for the repeated ascent of magmas [76–78]. Preserved cratonic regions (SCLMs) can be mapped as areas of high seismic velocity. At a global scale, it has been shown that smaller volumes of magmas directly originating from the mantle are positioned at the craton edge (Figure 4).

Domains of high seismic velocity can represent ancient blocks of metasomatized SLCM within a discrete mantle lithosphere domain flanked by major faults [63,64]. The IOCG Carajás province and Vale do Curaçá and Riacho do Pontal copper districts are located in the transition zone between domains of high and low velocities (Figure 4) and may reflect the refertilization of the SCLM and/or zones of higher lithospheric and mantle temperatures. Ore deposits that originate from the mantle or from transition mantle/crust magmas such as diamond, platinum-group elements (PGEs), Ni-Cu-(PGE), copper porphyry and IOCG deposits are situated along cratonic edges and can be related to the tectonic evolution of the SCLM [63,64,78]. In this context, the extensive gradients flanking either side of the high velocity zone through east-central Brazil should be evaluated in more detail (Figure 4).

Craton edges are characterized by a thinning of lithosphere and are strongly tectonized zones creating transtensional or transpressional sites along translithospheric faults [62]. These major shear or fault zones are frequently used for melt introduction into the crust. For example, IOCG districts in Australia, including the world class Olympic Dam in the Gawler craton and within the Eastern Succession of Mount Isa Inlier in Australia, are related to the presence of large igneous provinces (LIPs) that may contain a considerable amount of intrusive felsic rocks [8,10,71,79–83].

Fertile provinces that lead to the formation of mantle-related world-class deposits require melting of the SCLM on the margins of cratons, which is responsible for magmatic ascent associated high heat flow and volatile flow [25,65]. The deposits occur in long-lived subparallel regional structures that have been the focus of multiple reactivation events [24,26,28,30,34,47]. In the Riacho do Pontal and Vale do Curaçá Copper Districts, structural interpretations show that early thrust zones are reused several times and are overprinted by strike-slip shear zones [47].

7.1.2. Structural Control

Sigmoidal or "SC-shaped" structures are indicative of major shear systems [18,23,25,74,75]. Fractal patterns that mimic "SC" structures are systematically repeated from macro- to microscales. These structures serve as critical pathways for the upward flux of fluids promoting interactions between fluid and rock. Duplex, shear band, and asymmetrical structures are quite common along the shear system. The structural controls and traps used for orogenic gold in shear zones are the same as those used for IOCG deposits [24]. The more important traps for host orebodies include (a) interconnection zones between "SC" structures; (b) fractal second- or third-order "C" structures; (c) bends along shear zones in both horizontal and vertical planes where high-grade breccia are typically hosted; (d) fault intersections highly favorable for host breccia ores; and (e) ductile shear zones reactivated by late brittle faults that enrich older zones and that can generate new mineralized bodies. The permeability and degree of fluid overpressure (where fluid pressure > lithostatic pressure) greatly influence the formation of brecciated zones along shear zones.

Frequently, lithological boundaries between units with different competencies are crucial for hosting high deformation corridors. In this way, zones of contact with competent rocks such as paragneiss, mafic granulite, granulitic orthogneiss, and banded iron formations (BIFs) are usually trapped for the percolation of hydrothermal fluids related to shear zones. In the Vale do Curaçá copper district, considering only the epigenetic IOCG mineralization process, the host rocks are predominantly mafic and felsic granulitic rocks.

The orebodies often assume a sigmoidal shape, as they are often hosted in shear zones [8,11,70]. Often, early, sin and late-tectonic breccia pipe zones are found along hydrothermal IOCG systems. The evolution of IOCG-rich systems entails development by the direct melting of the SLCM, positioning in shear zones initially as pipe breccia, and continuous reworking by shear deformation. Variation in the direction and dipping along shear zones, both horizontally and vertically, acts as a structural trap for both hydrothermal and pipe breccias. Typically, breccia-rich ores are situated in a central hydrothermal system zone in transtensional structures.

7.1.3. Geophysical Implications for Alteration

Hydrothermal alteration is characterized by early high-temperature Na (albite) alteration (500–700 °C; [84]) to lower-temperature K-Fe (< 350 °C) alteration [20,24,27–29]. High-temperature albite alteration can be linked to magmatic-hydrothermal systems [26,82,84,85]. Iron is highly soluble at high temperatures and in saline fluids and is enhanced by increasing H^+ in the fluid system, resulting in more intense Fe fluxes [84].

Hydrothermal alteration is related to intermediate- to high-temperature fluids in the Riacho do Pontal and Vale do Curaçá districts. The alteration halo extends from 1 to 5 km in width, following the major shear zones. Sodic alteration is more distal and potassic, and calcic and ferric alterations are more proximal in both districts. The southern deposits and Sussuarana, Caraíba, and Surubim mines are related to deeper and high-temperature sodic/potassic hydrothermal alteration in contrast with the Vermelho deposit, in which hydrolytic alteration occurred in shallower zones in the IOCG hydrothermal system as initially described by [5,10]. Typically, a series of magnetic dipoles are linked to shear zones and hydrothermal halos.

The general hydrothermal zoning pattern for IOCG deposits is usually vertical from magnetite-dominant at depth to hematite-dominant at shallower levels [5,10,84–90]. Using this model, it is possible to interpret the Riacho do Pontal District as positioned in the shallowest portion of the IOCG system (Figure 14). Thus, additional work must be performed to identify deeper (or more eroded) areas of the IOCG system related to more magnetic and density targets, such as those identified in the Riacho Seco project.

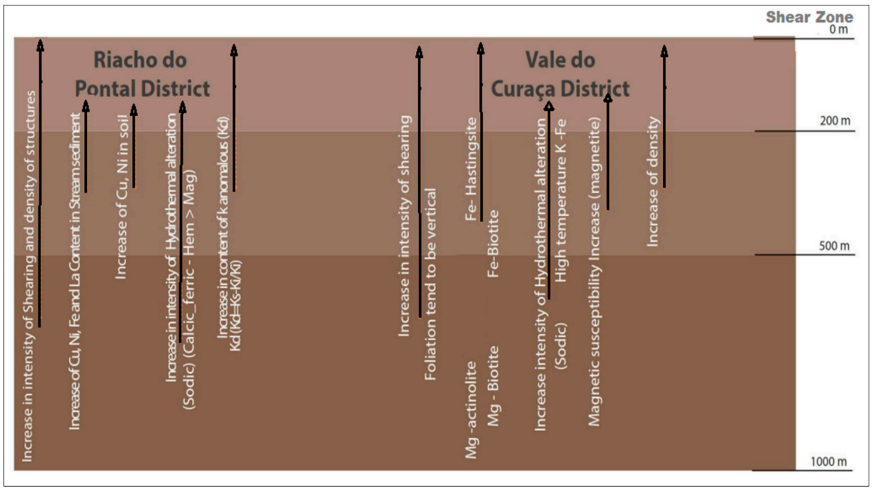

Figure 14. The main geological geochemical, structural, and geophysical vectors illustrating the footprint of the Vale do Curaçá and Riacho do Pontal Copper Districts (modified from [76]).

8. Exploration Potential

Through 2D and 3D mapping, it is possible to verify variation in these parameters with distance in the direction of mines, deposits, or occurrences. An increase or decrease in the intensity of these processes represents vectors towards the IOCG systems studied (Figure 14).

The main footprints of the two IOCG districts are described below:

Riacho do Pontal District:

(a) Structural: increase in shearing intensity and in the density of structures in the direction of secondary structures. Foliation tends to be vertical. Regardless of the structural regime, most deposits in both districts are controlled by bends in the host rocks.
(b) Stream sediment and soil: anomalies of Cu, Ni, Fe, and La in stream sediment and Cu (Ni, Ce and La) in soil.
(c) Low magnetic anomalies related to Kd (Kd-anomalous potassium) and shear zones [24].
(d) Low magnetic anomalies (abundant hematite related to ore zones).

Vale do Curaçá District:

(a) The district of Vale do Curaçá is associated regionally with high gravimetric and magnetic anomalies corresponding with the portion west of the ISCO.
(b) Our studied area is inboard of a relatively high velocity region, bordered eastwards by a low velocity region. The high-velocity region presumably indicates the cratonic area, with the lower velocity region demarcating the craton limit.
(c) The Caraíba mine bodies are strongly related to magnetic and gravimetric NS trends interpreted to have susceptibility with >0.09 SI and density >0 g/cm^3.

Hydrothermal alteration: an increase in the anomalies is related to hydrothermal processes: (i) distal sodic alteration and (ii) the mineralized zone intensely related to calcic-ferric alteration.

(d) Increases in Fe actinolite FeOt/and Fe-biotite (towards more hydrothermalized altered zones (Figure 14).

However, an atypical paradigm remains in the Vale do Curaçá district: the selection of new targets not necessarily hosted in ultramafic rocks. The IOCG system can develop in any host rock at varying depths. A full understanding of the IOCG model for mining companies can greatly expand exploration in the districts via data integration and the processing of structural, geological, and geophysical databases [11,65].

9. Conclusions

Knowledge of the signature of IOCG deposits in Brazil shows that these deposits can be hosted in any type of rock with specific styles of hydrothermal alteration and at different depths. Three-dimensional geological modeling, when combined with geophysical and structural interpretation, can facilitate the spatial and temporal understanding of the hydrothermal systems of the Vale do Curaça and Riacho do Pontal districts.

The main conclusions obtained from the present study of the Vale do Curaçá and Riacho do Pontal copper districts are as follows:

1. The Vale do Curaçá and Riacho do Pontal copper districts are hosted in distinct geological and tectonic settings, and an older IOCG mineralization event occurring within the São Francisco Craton is related to Palaeoproterozoic (ca 2 to 2.2 Ga) hydrothermal processes. A younger phase of IOCG mineralization in the Neoproterozoic (ca 750 to 570 Ma) has been recognized in the Brazilian mobile belt.
2. Both IOCG districts developed in an arc tectonic setting [50] overprinted by strike slip shear zones.

3. The interpretation of gravimetric and magnetic data shows different magnetic and gravimetric signatures for these two copper districts.
4. The Vale do Curaçá copper district is in a high regional gravimetric domain. It is 110 km in length and 22 km in width and shows a strong relationship with magnetic and gravimetric anomalies. The Caraíba, Surubim, and Vermelhos mines and some copper occurrences are positioned at this site.
5. The regional gravimetric signature of the Riacho do Pontal District is mainly related to a negative Bouguer NW–SE anomaly. This negative Bouguer anomaly represents the collisional suture between the cratonic block and mobile belt Riacho do Pontal. The IOCG occurrences of the Ria4 prospects are found in these low gravimetric signature domains. The rocks, slightly altered, have a density of 2.7–2.78 g/cm^3, and the most heavily altered rocks show densities of 2.75–3.1 g/cm^3.
6. The magnetic signatures are quite distinct. Copper corridors in the Vale do Curaçá copper district are associated with magnetic anomalies located in the western portion of the Itabuna-Salvador-Curaçá orogen. On the other hand, the copper deposits located in the belt of the Riacho do Pontal district are situated in zones with or without very weak magnetic anomalies.
7. MVI shows two main NNW prospective trends in the Vale do Curaça district. Trends I and II have a sigmoidal shear shape. These trends are positioned in the contact zone between domains with high magnetization (susceptibility > 0.005 SI) and density anomalies (>0 g/cm^3) and show a contrast in density and magnetite content. Trend I is 40 km in length and 10 km in width. It hosts the Caraíba, Surubim, and Vermelho mines and other deposits and is the most important trend for hosting IOCG deposits in the district.
8. The general hydrothermal zoning pattern for IOCG deposits is largely vertical from magnetite-dominant at depth to hematite-dominant in the upper levels. It is possible to interpret the Neoproterozoic Riacho do Pontal district as positioned in the shallowest portion of the IOCG system. Thus, additional work must be performed by searching for deeper (or more eroded) areas of the IOCG system related to more magnetic and dense areas (targets in the northern portion of the Riacho Seco target).
9. Large areas flanking the high-velocity seismic tomography image that already control, on a broad scale, the Carajás IOCG province and Riacho do Pontal and Vale do Curaçá copper districts in Brazil should be evaluated in more detail in a further exploratory program.

Author Contributions: Conceptualization, S.R.B.H. and A.M.S.; Methodology, A.M.S. and F.J.F.F.; Software, S.R.B.H.; Validation, A.M.S., C.B. and F.J.F.F.; Formal Analysis, C.B.; Investigation, S.R.B.H.; Resources, S.R.B.H.; Data Curation, A.M.S.; Writing-Original Draft Preparation, S.R.B.H.; Writing-Review & Editing, A.M.S. and C.B.; Visualization, S.R.B.H.; Supervision, A.M.S. and C.B.; Project Administration, A.M.S.; Funding Acquisition, A.M.S. All authors have read and agreed to the published version of the manuscript.

Funding: A.M. Silva gratefully acknowledges the National Council for Scientific and Technological Development (CNPq) for research grant 307177/2014-9.

Acknowledgments: The authors gratefully acknowledge Vale S. A. for supporting this study. We would like to thank the Vale exploration team for extensive discussions. We would also like to thank Victoria Basileu for providing special support in developing the figures.

Conflicts of Interest: The authors declare no conflict of interest related to the publication of this paper.

References

1. Hayward, N.; Corriveau, L.; Craven, J.A.; Enkin, R.J. Geophysical signature of the NICO Au-Co-Bi-Cu deposit and its iron oxide-alkali alteration system, Northwest Territories, Canada. *Econ. Geol.* **2016**, *111*, 2087–2109. [CrossRef]
2. Smith, R.J. Geophysics of iron oxide copper-gold deposits. In *Hydrothermal Iron Oxide Copper-Gold and Related Deposits*; Porter, T.M., Ed.; PGC Publishing: Adelaide, Australia, 2002; Volume 2, pp. 357–367.

3. Clark, D.A.; Geuna, S.; Schmidt, P.W. Predictive Magnetic Exploration Models for Porphyry, Epithermal and Iron Oxide Copper-Gold Deposits: Implications for Exploration, and Mining: Commonwealth Scientific and Industrial Research Organization (CSIRO) Exploration and Mining Report. 2013. 1073R. Available online: https://confluence.csiro.au/download/attachments/26574957/Clark%20etal%202004%20P700%20CSIRO%201073Rs.pdf?version=2&modificationDate=1460597746010&api=v2 (accessed on 24 November 2020).
4. Clark, D.A. Magnetic effects of hydrothermal alteration in porphyry copper and iron-oxide copper–gold systems: A review. *Tectonophysics* **2014**, *624–625*, 46–65. [CrossRef]
5. Hitzman, M.W.; Oreskes, N.; Einaudi, M.T. Geological characteristics and tectonic setting of proterozoic iron oxide (Cu U Au REE) deposits. *Precambrian Res.* **1992**, *58*, 241–287. [CrossRef]
6. Pollard, P.J.; Taylor, R.G.; Peters, L.; Matos, F.; Freitas, C.; Saboia, L.; Huhn, S. 40Ar-39Ar dating of Archean iron oxide Cu-Au and Paleoproterozoic granite-related Cu-Au deposits in the Carajás Mineral Province, Brazil: Implications for genetic models. *Miner. Deposita* **2018**, *54*, 329–346. [CrossRef]
7. Barton, M.D. *Iron Oxide (-Cu-Au-REE-P-Ag-U-Co) Systems: Treatise on Geochemistry*, 2nd ed.; 2014; Volume 13, pp. 515–541. Available online: https://doi.org/10.1016/B978-0-08-095975-7.01123-2 (accessed on 24 November 2020).
8. Groves, D.I.; Bierlein, F.P.; Meinert, L.D.; Hitzman, M.W. Iron oxide copper-gold (IOCG) deposits through earth history: Implications for origin, lithospheric setting, and distinction from other epigenetic iron oxide deposits. *Econ. Geol.* **2010**, *105*, 641–654. [CrossRef]
9. O'Driscoll, E.S.T. The application of lineament tectonics to the discovery of the Olympic Dam Cu-Au-U deposit at Roxby Downs, South Australia. *Glob. Tecton. Metallog.* **1985**, *3*, 43–57.
10. Hitzman, M.W. Iron oxide-Cu-Au deposits: What, where, when, and why. In *Hydrothermal Iron Oxide Copper-Gold and Related Deposits: A Global Perspective*; Porter, T.M., Ed.; Australian Mineral Foundation: Adelaide, Australia, 2000; pp. 9–25.
11. Groves, D.I.; Goldfarb, R.J.; Santosh, M. The conjunction of factors that lead to formation of giant gold provinces and deposits in non-arc settings. *Geosci. Front.* **2016**, *7*, 303–314. [CrossRef]
12. Hühn, S.R.B.; Nascimento, J.A.S. São os depósitos cupríferos de Carajás do tipo Cu-Au-U-ETR? In *Contribuições à Geologia da Amazônia*; Costa, M.L., Angélica, R.S., Eds.; FINEP.SBG-NO: Belém, Brazil, 1997; pp. 143–160.
13. Lindenmayer, Z.G. Evolução geológica do Vale do Rio Curaçá e dos corpos máfico-ultramáficos mineralizados a cobre (Orgs.). In *Geologia e Recursos Minerais do Estado da Bahia: Textos básicos*; Inda, H.A.V., Marinho, M.M., Duarte, F.B., Eds.; SME: Salvador, Brazil, 1981; Volume 4, pp. 72–110.
14. Lindenmayer, Z.G. Evolução Geológica do Vale do rio Curaçá e dos Corpos Máfico-Ultramáficos Mineralizados a Cobre. Master's Thesis, Universidade Federal da Bahia, Salvador, Brazil, 1982.
15. Requia, K.; Stein, H.; Chiaradia, M. Re-Os and Pb-Pb geochronology of the Archean Salobo iron oxide copper?gold deposit, Carajás mineral province, northern Brazil. *Miner. Depos.* **2007**, *38*, 727–738. [CrossRef]
16. Tallarico, F.H.B.; Figueiredo, B.R.; Groves, D.I.; Kositcin, N.; McNaughton, N.J.; Fletcher, I.R.; Rego, J.L. Geology and shrimp U-Pb geochronology of the igarape bahia deposit, carajas copper-gold belt, Brazil: An Archean (2.57 Ga) Example of Iron-Oxide Cu-Au-(U-REE) Mineralization. *Econ. Geol.* **2005**, *100*, 7–28. [CrossRef]
17. Dreher, A.M.; Xavier, R.P.; Taylor, B.E.; Martini, S.L. New geologic, fluid inclusion and stable isotope studies on the controversial Igarapé Bahia Cu–Au deposit, Carajás Province, Brazil. *Miner. Depos.* **2008**, *43*, 161–184. [CrossRef]
18. Monteiro, L.V.S.; Xavier, R.P.; De Carvalho, E.R.; Hitzman, M.W.; Johnson, C.A.; Filho, C.R.D.S.; Torresi, I. Spatial and temporal zoning of hydrothermal alteration and mineralization in the Sossego iron oxide–copper–gold deposit, Carajás Mineral Province, Brazil: Paragenesis and stable isotope constraints. *Miner. Depos.* **2008**, *43*, 129–159. [CrossRef]
19. Monteiro, L.V.S.; Caetano, J.; Souza, C.R.; Carvalho, E.R.; Hitzman, M.W. Mineral chemistry of ore and hydrothermal alteration at the Sossego iron oxide-copper-gold deposit, Carajás Mineral Province, Brazil. *Ore Geol. Rev.* **2008**, *34*, 317–336. [CrossRef]
20. Teixeira, J.B.G.; Silva, M.D.G.D.; Misi, A.; Cruz, S.C.P.; Sá, J.H.D.S. Geotectonic setting and metallogeny of the northern São Francisco craton, Bahia, Brazil. *J. S. Am. Earth Sci.* **2010**, *30*, 71–83. [CrossRef]

21. Xavier, R.P.; Rusk, B.; Emsbo, P.; Monteiro, L.V.S. Composition and source of salinity of ore-bearing fluids in Cu-Au systems of the Carajás Mineral Province, Brazil. In Proceedings of the 10th biennial meeting of the SGA, Townsville, Australia, 17–20 August 2009; Volume 1, pp. 272–274.
22. Xavier, R.P.; Monteiro, L.V.S.; Souza Filho, C.R.; Torresi, I.; Carvalho, E.R.; Dreher, A.M.; Wiedenbeck, M.; Trumbull, R.B.; Pestilho, A.L.S.; Moreto, C.P.N. The iron oxide copper-gold deposits of the Carajás Mineral Province, Brazil: An updated and critical review. In *Hydrothermal Iron Oxide Copper-Gold and Related Deposits: A Global Perspective, v3—Advances in Understanding of IOCG Deposits*; Porter, T.M., Ed.; PGC Publishing: Adelaide, Australia, 2010; pp. 285–306.
23. DeMelo, G.H.C.; Monteiro, L.V.S.; Xavier, R.P.; Moreto, C.P.N.; Santiago, E.S.B.; Dufrane, S.A.; Aires, B.; Santos, A.F.F. Temporal evolution of the giant Salobo IOCG deposit, Carajás Province (Brazil): Constraints from paragenesis of hydrothermal alteration and U-Pb geochronology. *Miner. Depos.* **2016**, *52*, 709–732. [CrossRef]
24. Hühn, S.R.B.; Silva, A.M. Favourability potential for IOCG type of deposits in the Riacho do Pontal Belt: New insights for identifying prospects of IOCG type deposits in NE Brazil. *Braz. J. Geol.* **2018**, *48*, 703–771. [CrossRef]
25. Holdsworth, R.; Pinheiro, R.V. The anatomy of shallow-crustal transpressional structures: Insights from the Archaean Carajás fault zone, Amazon, Brazil. *J. Struct. Geol.* **2000**, *22*, 1105–1123. [CrossRef]
26. Teixeira, J.B.G.; Silva, M.G.; Lindenmayer, Z.G.; Silva D'el-Rey, L.J.H.; Vasconcelos, P.M.; Reis, C.H.C.; Andrade, J.B.F. Depósitos de cobre do Vale do Rio Curaçá, Bahia. In *Modelos de Depósitos de Cobre do Brasil e Sua Resposta ao Intemperismo*; Brito, R.S.C., Silva, M.G., Kyumjian, R.M., Eds.; CPRM: Brasília, Brazil, 2010; p. 190.
27. Juliani, C.; Monteiro, L.V.; Fernandes, C.M.D. Potencial mineral: Cobre. In *Recursos Mineral do Brasil: Problemas e Desafios*; Academia Brasileira de Ciências: Rio de Janeiro, Brazil, 2016; pp. 134–153.
28. Huhn, S.R.B.; Sousa, M.J.; Filho, C.R.D.S.; Monteiro, L.V.S. Geology of the Riacho do Pontal iron oxide copper-gold (IOCG) prospect, Bahia, Brazil: Hydrothermal alteration approached via hierarchical cluster analysis. *Braz. J. Geol.* **2014**, *44*, 309–324. [CrossRef]
29. Garcia, P.M.D.P.; Teixeira, J.B.G.; Misi, A.; Sá, J.H.D.S.; Silva, M.D.G.D. Tectonic and metallogenic evolution of the Curaçá Valley Copper Province, Bahia, Brazil: A review based on new SHRIMP zircon U-Pb dating and sulfur isotope geochemistry. *Ore Geol. Rev.* **2018**, *93*, 361–381. [CrossRef]
30. D'el-Rey, L.J.H.; Oliveira, J.G.; Gaal, E.G. Implication of the Caraíba deposit's structural controls on the emplacement Brazilian. *J. Geol.* **1996**, *2*, 309–324.
31. Delgado, L.M.; Souza, J.D. *Projeto Cobre Curaçá. Cobre no Vale do Rio Curaçá, Estado da Bahia, Departamento Nacional de Produção Mineral, Seção Geologia Econômica*; Geologia Econômica: Brasilia, Brazil, 1981; pp. 7–149. (In Portuguese)
32. Mendonca, R.J. *Updated Mineral Resources and Mineral Reserves Statements of Mineração Caraíba's Vale do Curaçá Mineral Assets, Curaçá Valley*; Curaca Technical Report: Bahia, Brazil, 2018; p. 284. Available online: https://www.miningdataonline.com/reports/Curaca_Technical_report_2018.pdf (accessed on 24 November 2020).
33. Maier, W.D.; Barnes, S.J. The origin of Cu sulfide deposits at Curaçá Valley, Bahia, Brazil: Evidence from Cu, Ni, Se and platinum—Group element concentrations. *Econ. Geol.* **1999**, *2*, 165. [CrossRef]
34. Rocha, A.M.R. Metassomatismo Hidrotermal e Controle da Mineralização Aurífera na Área da Mina Futura, depósito de Caraíba, Bahia. Ph.D. Thesis, Universidade Federal do Rio Grande do Norte, Natal, Brazil, 1999.
35. Companhia Baiana De Pesquisa Minerais—CBPM. Informações Geológicas e de Recursos Minerais do Estado da Bahia. 2011. Available online: http://www.cbpm.com.br/igba (accessed on 24 November 2020).
36. Garcia, P.M.P. Metalogênese dos depósitos cupríferos de Caraíba, Surubim, Vermelhos e Sussuarana, Vale do Curaçá, Bahia, Brasil. Master's Thesis, Universidade Federal da Bahia, Salvador, Brazil, 2013.
37. Franklin, J.M.; Lydon, J.W.; Sangster, D.F. Volcanic associated massive sulfide deposits. In *Economic Geology, 75th Anniversary Volume*; Society of Economic Geologists: Denver, CO, USA, 1981; pp. 485–627.
38. Barrie, C.T.; Hannington, M.D. Introduction: Classification of VMS deposits based on host rock composition. In *Volcanic-associated massive sulfide deposits: Processes and Examples in Modern and Ancient Settings. Reviews in Economic Geology, n.8*; Society of Economic Geologists: Denver, CO, USA, 1999; pp. 2–10.
39. Delgado, L.M.; Sousa, J.D.; Projeto Cobre Curaçá. Geologia Econômica do Distrito Cuprífero do Rio Curaçá. In *Relatório Final*; CPRM: Salvador/Bahia, Brazil, 1975. Available online: http://rigeo.cprm.gov.br/jspui/handle/doc/8838 (accessed on 24 November 2020).

40. Fraguas, S. Evolução da Mina Caraíba, Bahia. In *Simexmin: Novos Casos de Sucesso em Exploração Mineral e Desenvolvimento de Minas no Brasil*; CD-ROM, V Simpósio Brasileiro de Exploração Mineral (Simexmin): Ouro Preto/MG, Brazil, 2012.
41. Barbosa, J.S.F. *The Granulites of the Jequié Complex and Atlantic Coast Mobile Belt, Southern Bahia, Brazil—An Expression of Archean/Early Proterozoic Plate Convergence*; Springer: Dordrecht, the Netherlands, 1990; pp. 195–221. Available online: https://link.springer.com/chapter/10.1007/978-94-009-2055-2_11 (accessed on 24 November 2020).
42. Barbosa, J.S.F.; Dominguez, J.M.L. (Eds.) *Geologia da Bahia: Texto Explicativo*; SGM: Salvador, Brazil, 1996; p. 400.
43. Padilha, A.V.; Melo, R.C. 8th Chapter. Evolução Geológica. In *PLGB. Pintadas. Folha SC-24-Y-D-V. Texto Explicativo*; Melo, R.C., Ed.; Escala 1:100.000. DNPM: Brasília, Brazil, 1991; pp. 129–157.
44. Barbosa, J.; Sabaté, P. Archean and Paleoproterozoic crust of the São Francisco Craton, Bahia, Brazil: Geodynamic features. *Precambrian Res.* **2004**, *133*, 1–27. [CrossRef]
45. Oliveira, E.P.; Windley, B.F.; McNaughton, N.J.; Pimental, M.; Fletcher, I.R. Contrasting copper and chromium metallogenic evolution of terranes in the Paleoproterozoic Itabuna-Salvador-Curaçá orogen, São Francisco Craton, Brazil: New zircon (SHRIMP) and SmeNd (model) ages and their significance for orogen-parallel escape tectonics. *Precambrian Res.* **2004**, *128*, 143–165. [CrossRef]
46. D'el-Rey, J.H.; Dantas, E.L.; Teixeira, J.B.G.; Laux, J.H.; Silva, M.G. U–Pb and Sm–Nd geochronology of amphibolites from the Curaçá Belt, São Francisco Craton, Brazil: Tectonic implications. *Gondwana Res.* **2007**, *12*, 454–467. [CrossRef]
47. Alves da Silva, F.C.; Chauvet, A.; Faure, M. Thrusting, wrench-type tectonics and granite emplacement during an early Proterozoic Basin closure: The example of the Itapecuru greenstone belt NE-Brasil. In *Anais II Simp. Geol. do Cráton do São Francisco*; Salvador. Soc. Bras. Geol: Núcleo Bahia/Sergipe, Brazil; pp. 63–66.
48. D'el-Rey, L.J.H. Geologia e controle estrutural do depósito cuprífero Caraíba, Vale do Curaçá, Bahia. Geologia e Recursos Naturais do Estado da Bahia, SME, 1985. *Série Textos Básicos* **1985**, *6*, 51–123.
49. Alkmin, F.F.; Brito Neves, B.; Castro, J.A. Arcabouço tectônico do Cráton São Francisco: Uma revisão. In *O Cráton do São Francisco*; Domingues, J.M.L., Misi, A., Eds.; SBG/SGM/CNPq: Salvador, Brazil, 1993; pp. 45–62.
50. Oliveira, R.G. Arcabouço geofísico, isostasia e causas do magmatismo cenozóico da Província Borborema e de sua margem continental (nordeste do Brasil). Ph.D. Thesis, Universidade Federal do Rio Grande do Norte, Natal, Brazil, 2008.
51. Jardim de Sá, E.F. A Faixa Seridó (Província Borborema, NE do Brasil) e o seu significado geodinâmico na Cadeia Brasiliana/Pan-Africana. Ph.D. Thesis, Universidade de Brasília, Brasília, Brazil, 1994; 803p.
52. Jardim de Sá, E.F.; Macedo, M.H.F.; Fuck, R.A. Terrenos proterozóicos na Província Borborema e a margem norte do Cráton São Francisco. *Rev. Bras. Geociências* **1992**, *4*, 472–480.
53. Gray, D.R.; Foster, D.A.; Meert, J.G.; Goscombe, B.D.; Armstrong, R.; Trouw, R.A.J.; Passchier, C.W. A Damara orogen perspective on the assembly of southwestern Gondwana. In *West Gondwana: Pre-cenozoic Correlations across the South Atlantic Region*; Pankhurst, R.J., Ed.; Geological Society Special Publications: London, UK, 2008; p. 294.
54. Liégeois, J.-P.; Stern, R.J. Sr–Nd isotopes and geochemistry of granite-gneiss complexes from the Meatiq and Hafafit domes, Eastern Desert, Egypt: No evidence for pre-Neoproterozoic crust. *J. Afr. Earth Sci.* **2010**, *57*, 31–40. [CrossRef]
55. Neves, B.B.D.B.; Fuck, R.A. The basement of the South American platform: Half Laurentian (N-NW)+half Gondwanan (E-SE) domains. *Precambrian Res.* **2014**, *244*, 75–86. [CrossRef]
56. De Araujo, C.E.G.; Rubatto, D.; Hermann, J.; Cordani, U.G.; Caby, R.; Basei, M.A.S. Ediacaran 2500-km-long synchronous deep continental subduction in the West Gondwana Orogen. *Nat. Commun.* **2014**, *5*, 5198. [CrossRef]
57. Ganade, C.E.; Cordani, U.G.; Agbossoumounde, Y.; Caby, R.; Basei, M.A.S.; Weinberg, R.F.; Sato, K. Tightening-up NE Brazil and NW Africa connections: New U–Pb/Lu–Hf zircon data of a complete plate tectonic cycle in the Dahomey belt of the West Gondwana Orogen in Togo and Benin. *Precambrian Res.* **2016**, *276*, 24–42. [CrossRef]
58. Grainger, C.J.; Groves, D.I.; Tallarico, F.H.; Fletcher, I.R. Metallogenesis of the Carajás Mineral Province, Southern Amazon Craton, Brazil: Varying styles of Archean through Paleoproterozoic to Neoproterozoic base- and precious-metal mineralisation. *Ore Geol. Rev.* **2008**, *33*, 451–489. [CrossRef]

59. Companhia Baiana De Pesquisa Minerais—CBPM. *Levantamento aerogeofísico Projeto Riacho Seco Andorinhas*; Companhia Baiana De Pesquisa Minerais—CBPM: Salvador, Brazil, 2001; 80p.
60. Reid, A.B. Aeromagetic survey design. *Geophysics* **1980**, *15*, 973–976. [CrossRef]
61. Ferreira, F.J.F.; De Souza, J.; Bongiolo, A.D.B.E.S.; De Castro, L.G. Enhancement of the total horizontal gradient of magnetic anomalies using the tilt angle. *Geophysics* **2013**, *78*, 33–41. [CrossRef]
62. Thompson, D.T. EULDPH: A new technique for making computer-assisted depth estimates from magnetic data. *Geophysics* **1982**, *47*, 31–37. [CrossRef]
63. Hinze, W.J.; von Frese, R.R.B.; Saad, A.H. *Gravity and Magnetic Exploration: Principles, Practices, and Applications*; Cambridge University Press: Cambridge, UK, 2013.
64. Begg, G.C.; Griffin, W.L.; Natapov, L.M.; O'Reilly, S.Y.; Grand, S.; O'Neill, C.J.; Poudjom Djomani, Y.; Deen, T.; Bowden, P. The lithospheric architecture of Africa: Seismic tomography, mantle petrology and tectonic evolution. *Geosphere* **2009**, *5*, 23–50. [CrossRef]
65. Begg, G.C.; Ronsky, A.M.H.; Arndt, N.T.; Griffin, W.L.G.; O'Reilly, S.Y.; Hayward, N. Lithospheric, cratonic and geodynamic setting of Ni-Cu-PGE sulphide deposits. *Econ. Geol.* **2010**, *105*, 1057–1070. [CrossRef]
66. Griffin, W.L.; Begg, G.C.; O'Reilly, S.Y. Continental-root control on the genesis of magmatic ore deposits. *Nat. Geosci.* **2013**, *6*, 905–910. [CrossRef]
67. Macleod, I.N.; Ellis, R.G. *Magnetic Vector Inversion, a Simple Approach to the Challenge of Varying Direction of Rock Magnetization*; Australian Society of Exploration Geophysicists, Extended Abstracts: Melbourne, Australia, 2013; pp. 1–4.
68. Telford, W.M.; Geldart, L.P.; Sheriff, R.E. *Applied Geophysics*, 2nd ed.; Cambridge University Press: Cambridge, UK, 1990.
69. Ellis, R.G.; de MacLeod, W.B. Inversion of Magnetic Data for Remanent and Induced Sources. ASEG Extended Abstracts. 2012, pp. 1–4. Available online: https://doi.org/10.1071/ASEG2012ab117 (accessed on 24 November 2020).
70. Oliveira, R.G.; Medeiros, V.C. Contrastes geofísicos e heterogeneidade crustal do terreno Pernambuco-Alagoas, Província Borborema, NE Brasil. In *SBG-Núcleo Nordeste. Simpósio de Geologia do Nordeste. 17*; Boletim: Recife, Brazil, 2000; Volume 16, p. 176.
71. Corriveau, L.; Mumin, A.H.; Setterfield, T. IOCG environments in Canada: Characteristics, geological vectors to ore and challenges. In *Hydrothermal Iron Oxide Copper-Gold & Related Deposits: A Global Perspective*; Porter, T.M., Ed.; Porter Geoscience Consultancy Publishing: Adelaide, Australia, 2010; Volume 4, pp. 311–344.
72. Potter, E.G.; Corriveau, L.; Kerswill, J.K. Potential for iron oxide-copper–gold and affiliated deposits in the proposed national park area of the East Arm, Northwest Territories: Insights from the Great Bear magmatic zone and global analogs. In *Mineral and Energy Resource Assessment for the Proposed Thaidene Nene National Park Reserve, East Arm of Great Slave Lake, Northwest Territories*; Wright, D.F., Ed.; Open File 7196; Geological Survey of Canada: Ottawa, ON, Canada, 2013.
73. Braitenberg, C. Exploration of tectonic structures with GOCE in Africa and across-continents. *Int. J. Appl. Earth Obs. Geoinf.* **2015**, *35*, 88–95. [CrossRef]
74. Haddad-Martim, P.M.; Carranza, E.J.M.; Filho, C.R.D.S. The Fractal Nature of Structural Controls on Ore Formation: The Case of the Iron Oxide Copper-Gold Deposits in the Carajás Mineral Province, Brazilian Amazon. *Econ. Geol.* **2018**, *113*, 1499–1524. [CrossRef]
75. Costa, I.A. *Aerogeofísica em Carajás pelo Serviço Geológico do Brasil*; CPRM Serviço Geologico do Brasil: Brasília, Brasil, 2017; p. 5. Available online: www.cprm.gov.br (accessed on 24 November 2020).
76. Lesher, M.; Hannington, M.; Galley, A.; Ansdell, K.; Astic, T.; Banerjee, N.; Beauchamp, S.; Beaudoin, G.; Bertelli, M.; Beyer, S.; et al. Integrated multi-parameter exploration footprints of the Canadian Malartic disseminated Au, McArthur River-Millennium unconformity U, and Highland Valley porphyry Cu deposits: Preliminary results from the NSERC-CMIC Footprints Research Network. In *Conference Proceedings for Exploration 17: Exploration in the New Millennium, Sixth Decennial International Conference on Mineral Exploration*; Tschirhart, V., Thomas, M.D., Eds.; Conferências Decenais de Exploração Mineral: University Avenue Toronto, ON, Canada, 2017; pp. 325–347.
77. Barnett, C.T.; Williams, P.M. A radical approach to exploration: Let the data speak for themselves. *Soc. Econ. Geol. Newsl.* **2012**, *1*, 12–17.

78. Cooke, D.R.; Baker, M.; Hollings, P.; Sweet, G.; Chang, Z.; Danyushevsky, L.; Gilbert, S.; Zhou, T.; White, N.C.; Gemmell, J.B.; et al. New advances in detecting the distal geochemical footprints of porphyry systems—Epidote mineral chemistry as a tool for vectoring and fertility assessments. *Soc. Econ. Geol. Spec. Publ.* **2014**, *18*, 127–152.
79. Griffin, W.L.; O'Reilly, S.Y.; Afonso, J.C.; Begg, G.C. The Composition and Evolution of Lithospheric Mantle: A Re-evaluation and its Tectonic Implications. *J. Pet.* **2008**, *50*, 1185–1204. [CrossRef]
80. Czarnota, K.; Hoggard, M.J.; White, N.; Winterbourne, J. Spatial and temporal patterns of Cenozoic dynamic topography around Australia. *Geochem. Geophys. Geosystems* **2013**, *14*, 634–658. [CrossRef]
81. Pirajno, F.; Bagas, L. A review of Australia's Proterozoic mineral systems and genetic models. *Precambrian Res.* **2008**, *166*, 54–80. [CrossRef]
82. McPHIE, J.; Kamenetsky, V.S.; Allen, S.; Courtney-Davies, L.; Agangi, A.; Bath, A. The fluorine link between a supergiant ore deposit and a silicic large igneous province. *Geology* **2011**, *39*, 1003–1006. [CrossRef]
83. Pirajno, F.; Hoatson, D.M. A review of Australia's Large Igneous Provinces and associated mineral systems: Implications for mantle dynamics through geological time. *Ore Geol. Rev.* **2012**, *48*, 2–54. [CrossRef]
84. Oliver, N.H.S. Modelling the role of sodic alteration in the genesis of iron-oxide copper-gold deposits, Eastern Mt Isa Block, Australia. *Econ. Geol.* **2004**, *99*, 1145–1176. [CrossRef]
85. Pollard, P.J. An intrusion-related origin for Cu–Au mineralization in iron oxide–copper–gold (IOCG) provinces. *Miner. Depos.* **2006**, *41*, 179–187. [CrossRef]
86. Williams, P.J. Iron mobility during synmetamorphic in the Selwyn Range area, NW Queensland: Implications for the origin of iron-stone-hosted Au-Cu deposits. *Miner. Depos.* **1994**, *29*, 250–260. [CrossRef]
87. McCafferty, A.E.; Phillips, J.D.; Driscoll, R.L. Magnetic and Gravity Gradiometry Framework for Mesoproterozoic Iron Oxide-Apatite and Iron Oxide-Copper-Gold Deposits, Southeast Missouri. *Econ. Geol.* **2016**, *111*, 1859–1882. [CrossRef]
88. Leão-Santos, M.; Li, Y.; Moraes, R. Application of 3D magnetic amplitude inversion to iron oxide-copper-gold deposits at low magnetic latitudes: A case study from Carajás Mineral Province, Brazil. *Geophysics* **2015**, *80*, B13–B22. [CrossRef]
89. Belperio, A.; Flint, R.; Freeman, H. Prominent Hill: A hematite-dominated, iron oxide copper-gold system. *Econ. Geol.* **2007**, *102*, 1499–1510. [CrossRef]
90. Skirrow, R. The Olympic IOCG province (Gaoler craton): Lithospheric to district-scale controls on ore formation, and targeting of IOCG mineral systems. In Proceedings of the Geoconferences IOCG Workshop, Perth, Australia, 29 May 2014; Available online: http://geoconferences.org.au/wp-content/uploads/PR_TeamWA_R_Skirrow.pdf (accessed on 24 November 2020).